Activation of Different Cl Currents in *Xenopus* Oocytes by Ca Liberated from Stores and by Capacitative Ca Influx

H. CRISS HARTZELL

From the Department of Anatomy and Cell Biology, Emory University School of Medicine, Atlanta, Georgia 30322-3030

ABSTRACT *Xenopus* oocytes are an excellent model system for studying Ca signaling. The purpose of this study was to characterize in detail the Ca-activated Cl currents evoked by injection of inositol 1,4,5-trisphosphate (IP_3) into *Xenopus* oocytes voltage-clamped with two microelectrodes. Injection of IP_3 into *Xenopus* oocytes activates two different Ca-activated Cl currents. $I_{Cl\text{-}1}$ is stimulated rapidly (within 5 s after IP_3 injection), exhibits time-dependent activation upon depolarization, a linear instantaneous IV relationship with a reversal potential near E_{Cl}, and a curvilinear activation curve with an approximate half-maximal activation voltage of >200 mV. $I_{Cl\text{-}2D}$ is stimulated slowly after IP_3 injection (half-maximal stimulation occurs ~3 min after injection). $I_{Cl\text{-}2D}$ has a strongly outwardly rectifying instantaneous IV relationship with a reversal potential near E_{Cl} and is activated by hyperpolarization with a half-maximal activation voltage of −105 mV. $I_{Cl\text{-}2D}$ cannot be activated by Ca released from stores but is activated by Ca influx. In contrast, $I_{Cl\text{-}1}$ can be stimulated by Ca released from intracellular Ca stores. It can also be stimulated by Ca influx through store-operated channels if the Ca driving force is increased by a hyperpolarization immediately before the depolarization that gates $I_{Cl\text{-}1}$ channels. The description of two currents activated by influx and Ca release from stores provides new insights into and questions about the regulation of Ca in *Xenopus* oocytes.
Key words: *Xenopus* oocytes • inositol phosphate • Cl channels • calcium • Ca channels

INTRODUCTION

The concentration of cytosolic free Ca ($[Ca]_i$) regulates many physiological processes. These processes are controlled by receptors that activate Ca release from intracellular stores or increase Ca influx from the extracellular space (Tsien and Tsien, 1990; Pozzan et al., 1994; Clapham, 1995). Ca is mobilized from internal stores by inositol 1,4,5-trisphosphate (IP_3)[1] produced by activation of many G-protein–coupled and tyrosine kinase–coupled receptors that stimulate phospholipase C. Release of Ca from internal stores is often followed by a sustained influx of extracellular Ca (Putney, 1990; Meldolesi et al., 1991; Putney, 1992; Putney, 1993; Fasolato et al., 1994). This influx ("capacitative Ca entry") is mediated by store-operated Ca channels (SOCCs) in the plasmalemma that are apparently controlled by the level of Ca in the internal store.

The activation of a Ca influx pathway subsequent to Ca liberation from stores has been demonstrated by showing that activation of PLC-coupled receptors produces only a transient increase in cytosolic Ca concentration when the cell is bathed in zero Ca solution, but addition of extracellular Ca results in a large sustained increase in intracellular Ca (Takemura and Putney, 1989; Putney, 1992). The Ca influx is thought to be stimulated by "depletion" of internal stores because a similar Ca influx is stimulated by other interventions that lower store Ca. Ca-ATPase inhibitors thapsigargin, cyclopiazonic acid, and BHQ as well as intracellular bis(*o*-aminophenoxy)ethane-N,N,N′,N′-tetracetic acid (BAPTA) deplete Ca stores passively by preventing reuptake of Ca that leaks out (see Pozzan et al., 1994). The Ca ionophore ionomycin at low concentrations can deplete stores and activate capacitative Ca entry without directly affecting the plasma membrane (Morgan and Jacob, 1994). Store-operated Ca channels are not opened directly by IP_3 or Ca, because Ca ATPase inhibitors and ionomycin do not stimulate IP_3 production, and BAPTA prevents elevation of cytosolic Ca.

Xenopus oocytes have been a very useful model system for studying calcium signaling partly because these cells express Ca-activated Cl channels that can be used as real-time indicators of cytosolic Ca concentration (Dascal, 1987) and partly because their large size facilitates the study of spatial and temporal changes in cytosolic Ca concentrations (Girard and Clapham, 1993; Lechleiter and Clapham, 1992). For the past year, we have been using *Xenopus* oocytes as a heterologous expression system for putative store-operated Ca channels and have used the endogenous Ca-activated Cl currents as an indirect assay of cytosolic Ca concentrations. These Cl currents have been studied extensively by others (see Dascal [1987] and references in DISCUSSION). However, we found that the behavior of these currents was more complex than we anticipated and found it necessary to undertake a more detailed, quantitative

Address correspondence to H. Criss Hartzell, Department of Anatomy and Cell Biology, Emory University School of Medicine, Atlanta, Georgia 30322-3030. Fax: 404-727-6256; E-mail: criss@anatomy.emory.edu

[1] *Abbreviations used in this paper:* IP_3, inositol 1,4,5-trisphosphate, BAPTA, bis(*o*-aminophenoxy)ethane-N,N,N′,N′-tetracetic acid.

J. GEN. PHYSIOL. © The Rockefeller University Press • 0022-1295/96/09/157/19 $2.00
Volume 108 September 1996 157–175

analysis of them in order to interpret our results with heterologously expressed channels. In our analysis, we have found that there are two distinct Ca-activated Cl currents in *Xenopus* oocytes and that one current is activated preferentially by Ca influx through store-operated channels and that the other can be activated both by Ca influx and by Ca release from internal stores. Because these currents are dually regulated by voltage and by Ca, interpretation of effects of elevation of cytosolic Ca can be complicated.

METHODS

Electrophysiological Methods

Xenopus oocytes were voltage-clamped with two-microelectrodes using a GeneClamp 500 (Axon Instruments, Foster City, CA). Electrodes were filled with 3 M KCl and had resistances of 1–2 MΩ. Typically, the membrane was held at −35 mV, and voltage steps were applied as described in the text. Stimulation and data acquisition were controlled by PClamp 6.01 (Axon Instruments) via a Digidata 1200 A/D–D/A converter (Axon Instruments) and a Gateway P5-90 computer (Intel Pentium, 90 MHz). During recording, the oocyte was superfused with normal Ringer solution. The bath chamber volume was ~300 μl and was superfused at a rate of 2 ml/min unless the composition of the solution was being changed, in which case superfusion rates as high as 15 ml per min were used. When the composition of the bath was to be changed, the superfusion rate of the control solution was increased for several minutes before changing to the new solution at the same flow rate. Experiments were performed at room temperature (22–26°C).

Microinjection

Oocytes were injected with IP_3 or BAPTA using a Nanoject Automatic Oocyte Injector (Drummond Scientific Co., Broomall, PA). The injection pipet was pulled from glass capillary tubing in a manner similar to the recording electrodes and then broken so that it had a beveled tip with an inside diameter of <20 μm. Typically, 4.6 nl of a 10 mM solution IP_3 in H_2O was injected to give a calculated oocyte concentration of ~50 μM. The Ca concentration in this solution was not buffered, but injection of H_2O produced no change in membrane current. Usually we injected 23 nl of a 50 mM solution of K_4·BAPTA in water to give a final calculated concentration in the oocyte of 1 mM. The injection pipets were usually left impaled in the oocyte for the duration of the experiment, unless the oocyte was injected with two different solutions, in which case the first pipet was withdrawn before the second pipet was inserted.

Solutions

Normal Ringer consisted of 123 mM NaCl, 2.5 mM KCl, 1.8 mM $CaCl_2$, 1.8 mM $MgCl_2$, 10 mM HEPES, pH 7.4, 5 mM glucose, 5 mM sodium pyruvate. Zero Ca Ringer was the same except $CaCl_2$ was omitted, $MgCl_2$ was increased to 5 mM, and 0.1 mM EGTA was added. For 10 mM Ca Ringer, $CaCl_2$ was increased to 10mM.

Harvesting Eggs

Stage V-VI oocytes were harvested from adult *Xenopus laevis* females (Xenopus I) as described by Dascal (Dascal, 1987). *Xenopus* were anesthetized by immersion in Tricaine (1.5 g/liter). Ovarian follicles were removed, cut into small pieces, and digested in normal Ringer with no added calcium containing 2 mg/ml collagenase type IA (Sigma Chemical Co., St. Louis, MO) for 2 h at room temperature. The oocytes were extensively rinsed and placed in L15 medium (Gibco BRL, Gaithersburg, MD) and stored at 18°C. Oocytes were usually used between 1 and 6 d after isolation.

Display and Analysis of Data

For display of the figures, current transients during voltage steps were either blanked for 4 ms (e.g., see Fig. 2 *B*) or 4 ms of the data was replaced with the value of the current immediately before the voltage step (e.g., see Fig. 3 *B*). Data points are the mean and error bars are ±SEM. Each current-voltage and activation

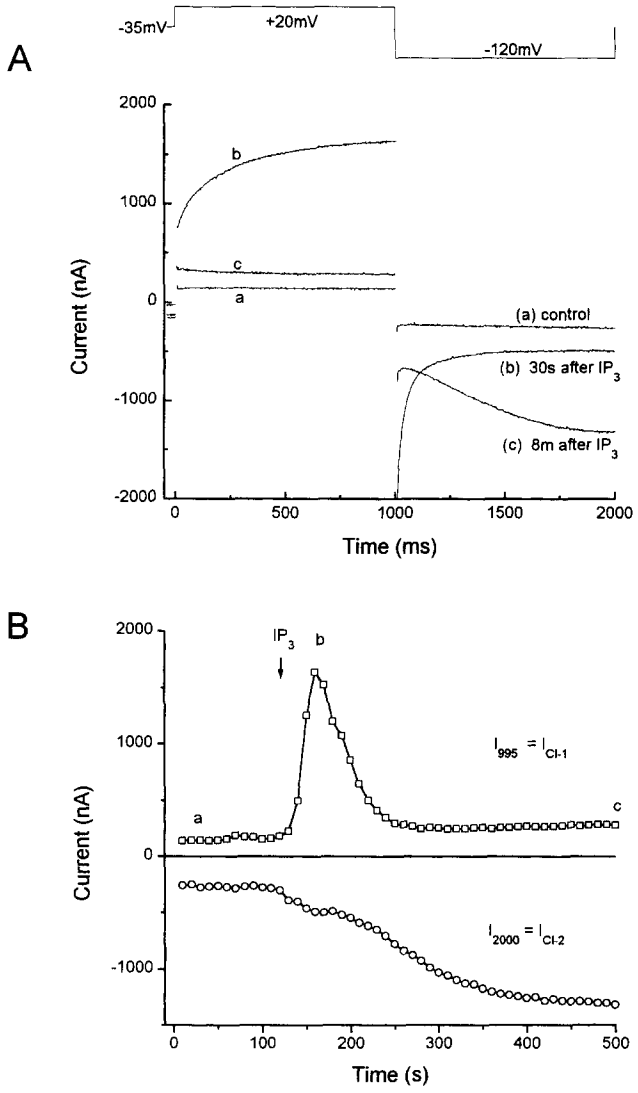

FIGURE 1. Effects of intracellular injection of IP_3 on ionic currents in *Xenopus* oocytes. (*A*) Current responses to 1-s voltage step to +20 mV followed by 1-s step to −120 mV from a holding potential of −35 mV. Trace *a* is before, trace *b* 30 s after, and trace *c* 8 min after IP_3 injection. (*B*) Time course of change in current at end of +20 mV pulse (I_{995}) and at end of −120 mV pulse (I_{2000}) as a function of time after injection of IP_3. IP_3 was injected at the arrow. The letters *a*, *b*, and *c* correspond to the traces in *A*.

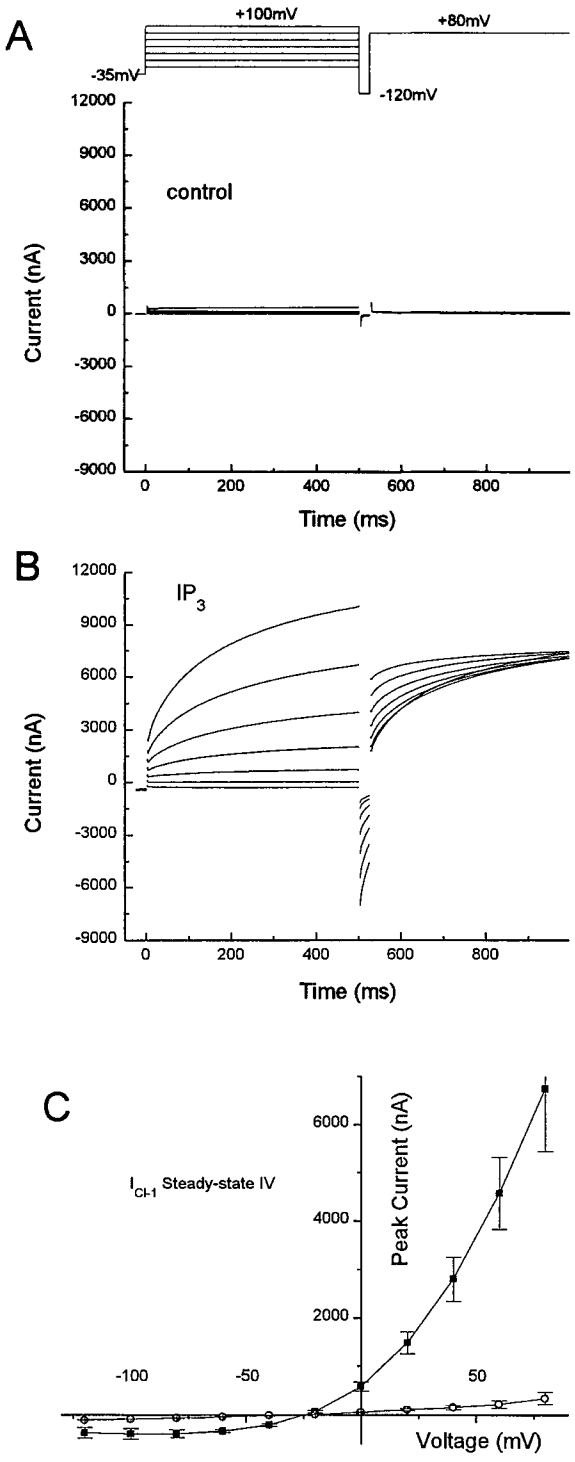

FIGURE 2. Steady-state IV relationship of $I_{Cl\text{-}1}$. The oocyte was stepped from −60 mV to different potentials between −40 and +100 mV for 500 ms followed by a step to −120 mV for 50 ms and a 500 ms step to +80 mV as shown. (*A*) Steady-state IV traces before IP_3 injection. (*B*) Steady-state IV traces after IP_3 injection. (*C*) Average steady-state IV relationship for six oocytes before (*open circles*) and after (*solid squares*) IP_3 injection. The currents at the end of the first voltage pulses (at 495 ms) were plotted vs. the test potential. This curve was constructed from two different voltage protocols. The first protocol was identical to the one shown in *A* and *B*. The other was similar, except that the holding potential was −120 mV and the test voltage steps were from −120 to +80. In the voltage range where these two protocols overlapped (−40 to +80 mV) the data points were identical within <10%, so the data were pooled.

curve is the average of three to six different oocytes. For current-voltage relationships, the raw data was averaged. For the activation curves, the data was normalized such that the current at a particular voltage was set as 1.0. Mathematical fits were performed using an iterative Levenberg-Marquardt algorithm. Unless noted, the interval between stimuli was 10–20 s. In tail current analysis, one would like to be able to measure the current immediately after the voltage step, but because of the capacitative transient, we were not able to measure the instantaneous current sooner than 4 ms after the step. However, this error seems unlikely to contribute significantly to our conclusions because experiments where we carefully subtracted capacitative transients provided the same IV curves as the ones where current was measured at 4 ms.

RESULTS

IP_3 Injection Activates Two Currents with Different Kinetics

Fig. 1 shows the effect of injecting 4.6 nl of 10 mM IP_3 to produce a calculated intraoocyte IP_3 concentration of ~50 μM. The standard voltage protocol for these experiments was a 1-s duration pulse from a −35 mV holding potential to +20 mV followed by a 1-s duration pulse to −120 mV. The voltage pulse under basal conditions produced only small time-independent currents (Fig. 1 *A*, *a*). However, immediately after injecting IP_3, an outward current was elicited by the +20 mV pulse (Fig. 1 *A*, *b*). This current exhibited two components, an instantaneous increase followed by a slowly developing outward current. As shown below, these two components were attributed to the same current: the instantaneous component reflected increased current (due to the increased driving force) through channels that were already open at −35 mV, and the time-dependent component reflected voltage-dependent opening of additional channels. The time-dependent component was well-fitted with two exponentials with τ = 28 and 274 ms at +20 mV. Upon repolarization to −120 mV, a tail current was observed that rapidly but incompletely inactivated with τ = 17 and 67 ms. This tail current was due to the voltage-dependent closing of channels that were open at +20 mV. This outward current and its associated tail current was named $I_{Cl\text{-}1}$ We believe that this current is a Ca-activated Cl current that is induced by Ca released from intracellular stores by the injected IP_3. Our reasons for this conclusion are based on the observations that $I_{Cl\text{-}1}$ (*a*) was blocked by 0.5 mM niflumic acid (a Ca-activated Cl channel blocker [White and Aylwin, 1990]), (*b*) had a reversal potential near the Cl equilibrium potential, and (*c*) its induction was independent of extracellular Ca and was unaffected by extracellular La, Ba, or Mn. These data are shown below.

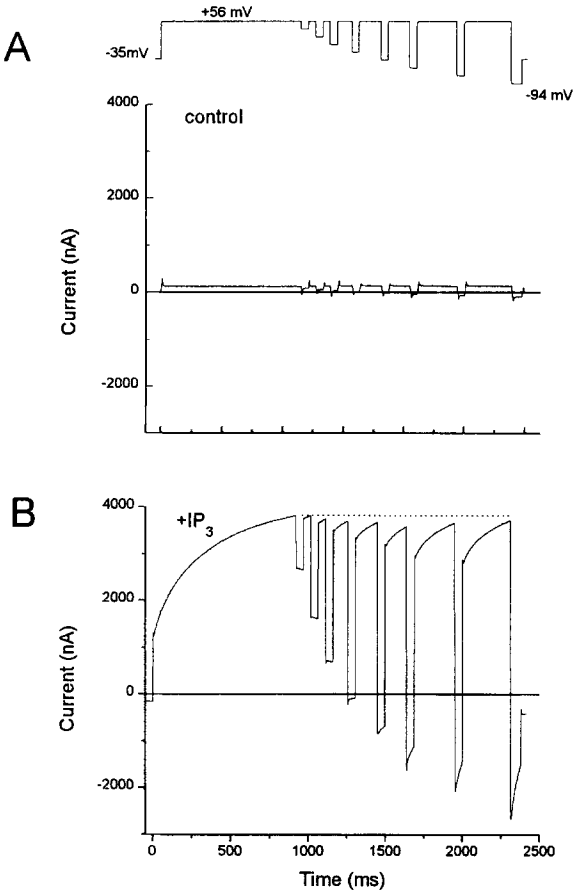

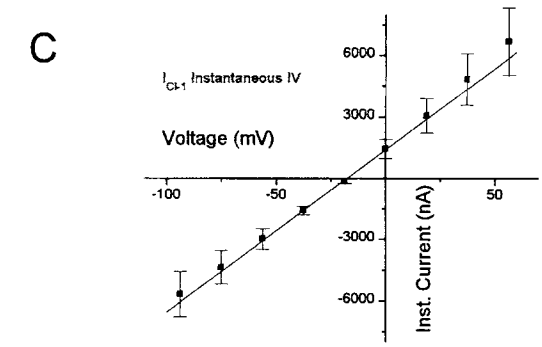

FIGURE 3. Instantaneous IV relationship of $I_{Cl\text{-}1}$. The oocyte was stepped from −35 to +60 mV for 500 ms followed by short repolarizations of 50 ms to different test potentials between +50 and −100 mV. (*A*) IV traces before IP_3 injection. (*B*) IV traces after IP_3 injection. (*C*) Average instantaneous IV relationship for four oocytes determined as shown in *B*. The current was measured at 4 ms after the start of the test pulses.

Over the next several minutes, the $I_{Cl\text{-}1}$ outward current and its inward tail current became smaller in amplitude. Concurrent with the decrease in $I_{Cl\text{-}1}$, a time-dependent inward current developed in response to the voltage step to −120 mV. This current exhibited a sigmoid onset and was fitted well by an exponential of the form $I = I_0 + A^*[1 - \exp(-x/\tau)]^p$ where $p = 2$ and $\tau = 289$ ms. This inward current was not accompanied by a significant outward current at +20 mV using this protocol. This inward current was named $I_{Cl\text{-}2}$. This current was also a Ca-activated Cl current, as it was blocked by 0.5 mM niflumic acid and had a reversal potential that coincided with the Cl equilibrium potential. However, this current required influx of extracellular Ca to be activated as described below.

The time course of development and decay of $I_{Cl\text{-}1}$ and $I_{Cl\text{-}2}$ are shown in Fig. 1 *B*. In this plot, $I_{Cl\text{-}1}$ was measured as the current at the end of the +20 mV pulse, and $I_{Cl\text{-}2}$ was measured at the end of the −120 mV pulse. $I_{Cl\text{-}1}$ developed fully within 30 s after injection of IP_3 and then declined nearly to baseline in ~1.5 min. $I_{Cl\text{-}2}$ developed slowly and was not maximally activated until >5 min after IP_3 injection.

$I_{Cl\text{-}1}$ Is a Cl Current with a Linear Instantaneous Current-Voltage Relationship

Steady-state IV relationship. The "steady-state" IV curve for $I_{Cl\text{-}1}$ was determined using the protocol shown in Fig. 2, *A* and *B*. The cell was depolarized to different command potentials for 500 ms from a holding potential of −35 mV before (Fig. 2 *A*) or immediately after (Fig. 2 *B*) injection of IP_3. The amplitude of the outward current at the end of the command pulse was

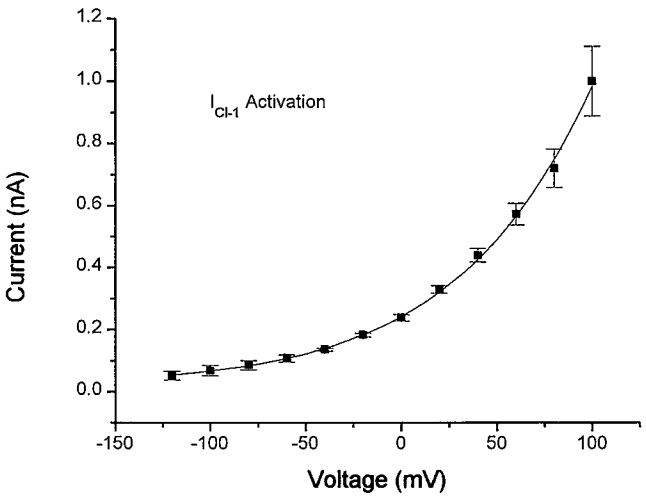

FIGURE 4. Activation curve of $I_{Cl\text{-}1}$. The activation curve was determined using the protocol shown in Fig. 2, *A* and *B*. $I_{Cl\text{-}1}$ was activated by 500-ms duration prepulses to different potentials. The activation curve was then determined by measuring the current 4 ms after hyperpolarizing to a test potential of −120 mV and plotted as a function of the prepulse potential. As described in the legend to Fig. 2 *C*, this curve was constructed from two slightly different protocols (holding potentials of −60 mV or −120 mV). In the region where these protocols overlapped, the curves were identical within <10%. The data were fitted to the Boltzmann equation: $I = 7.94/[1 + \exp^{(V - 226)/64}] + 7.96$.

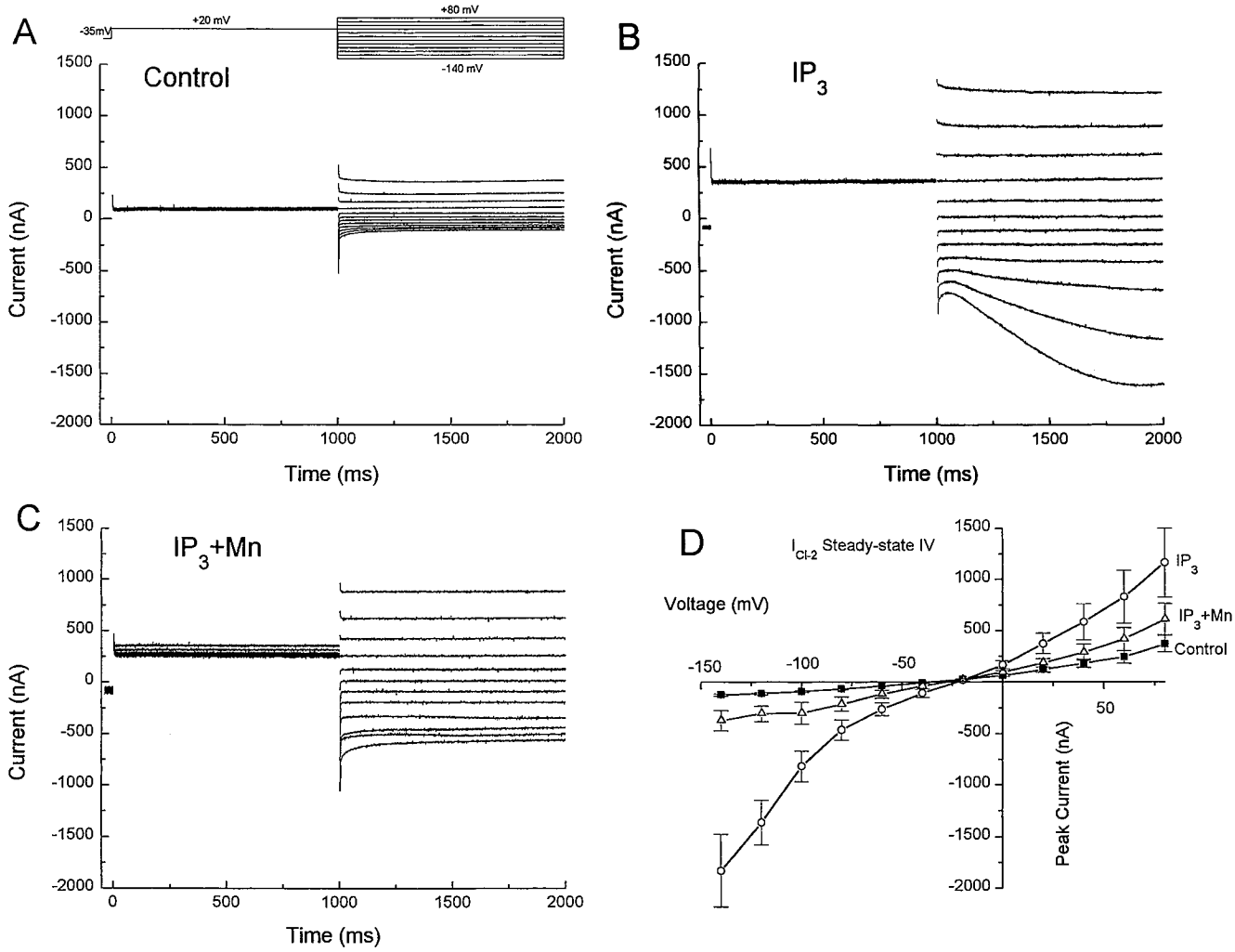

FIGURE 5. Steady-state IV relationship for $I_{Cl\text{-}2}$. Steady state IV relationship was determined by giving a 1-s duration pulse from a holding potential of −35 to +20 mV followed by a 1-s test pulse to different potentials. (*A*) IV traces before IP_3 injection. (*B*) IV traces ~15 min after IP_3 injection. (*C*) IV traces after IP_3 injection and addition of 1 mM $MnCl_2$ to the bath. (*D*) Average steady-state IV relationship from four cells measured as shown in *A–C*. The current at 1,995 ms was plotted vs. test potential. Before IP_3 injection (*solid squares*), ~15 min after IP_3 injection (*open circles*), and after IP_3 injection with Mn added to the bath (*open triangles*).

plotted vs. the command potential to give the steady-state IV curve (Fig. 2 *C*). The curve in Fig. 2 *C* is the average of four oocytes, but each individual oocyte had an IV curve with the same shape. The $I_{Cl\text{-}1}$ steady-state IV curve rectified strongly in the outward direction (Fig. 2 *C*). A problem we encountered in performing these experiments was that the amplitude of $I_{Cl\text{-}1}$ changed quickly after injecting IP_3 (Fig. 1 *B*). To measure the IV curve quickly while $I_{Cl\text{-}1}$ was not changing significantly, pulses were given at 2-s intervals. Further, to verify that the amplitude of $I_{Cl\text{-}1}$ had not changed during the run, the membrane was stepped to +80 mV for 500 ms at the end of each trial to verify that $I_{Cl\text{-}1}$ amplitude at this given voltage was the same for all trials. In Fig. 2 *B*, the amplitude of $I_{Cl\text{-}1}$ at 950 ms was the same for all the trials.

The current (I) plotted in Fig. 2 *C* is equal to:

$$I = N \cdot p_o \cdot \gamma \cdot (E_m - E_{rev}),$$

where N is the number of available channels, p_o is the channel open probability, γ is single channel conductance, E_m is membrane potential, and E_{rev} is the reversal potential of the current. To determine which of these terms might contribute to the rectification, we measured the instantaneous IV curve of $I_{Cl\text{-}1}$ as shown in Fig. 3.

Instantaneous IV relationship. To measure the IV relationship, the membrane was stepped to 60 mV for 500 ms to activate $I_{Cl\text{-}1}$ and then was hyperpolarized to different test potentials for 50 ms (Fig. 3, *A* and *B*). If we assume that only the driving force ($E_m - E_{rev}$) changed instantaneously, the initial amplitude at the onset of

the test pulse is equal to the current through the channels that were open at the end of the 60-mV command pulse. The instantaneous current was plotted vs. the potential of the test pulse. The interval between hyperpolarizing pulses was adjusted to the minimum required for $I_{Cl\text{-}1}$ to return to its fully activated amplitude (*dotted horizontal line* in Fig. 3 *B*) before the next hyperpolarizing pulse. The initial amplitude of the tail current was then plotted vs. the test potential. Before IP_3 injection, only very small current responses were recorded in response to the voltage pulses (Fig. 3 *A*). However, after IP_3 injection, the hyperpolarizing pulses produced large current responses (Fig. 3 *B*). The average instantaneous IV curve for $I_{Cl\text{-}1}$ recorded from four oocytes (Fig. 3 *C*) was essentially linear and had a reversal potential very close to the calculated Cl equilibrium potential (−20 mV) (Dascal, 1987). The fact that the instantaneous IV curve was essentially linear suggested that the rectification of the steady-state IV was not due to rectification of current through open channels. This suggested that voltage-dependent gating of the channel was responsible for rectification.

Activation curve. To test this hypothesis, we measured the activation curve of $I_{Cl\text{-}1}$ using the same protocol shown in Fig. 2, *A* and *B*. In this protocol, a different number of channels were activated by stepping to different command potentials between −40 mV and +100 mV for 500 ms. The membrane was then repolarized to a test potential of −120 mV for 50 ms, and the initial amplitude of the tail current was measured. We also used a similar protocol with a larger command potential range of −120 to 80 mV. Because the amplitude of the tail current was always measured at the same potential, $E_m - E_{rev}$ was constant. We assumed that γ did not change instantaneously as a function of voltage, therefore this measurement predicted the fraction of channels open at different voltages. These data showed the activation of $I_{Cl\text{-}1}$ increased with depolarization, but the current was not maximally activated even with command potentials as high as +100 mV (Fig. 4). The data in Fig. 4 fitted to the Boltzmann equation suggested that the half-activation potential was +226 mV, although the precision of the parameters derived from this fit should be viewed with some skepticism.

Thus, the steady-state IV of $I_{Cl\text{-}1}$ outwardly rectified because of the voltage dependence of channel activation, but the current through the open channels had approximately a linear current-voltage relationship.

$I_{Cl\text{-}2}$ Is a Cl Current with a Strongly Outwardly Rectifying Instantaneous IV Relationship

Steady-state IV relationship. Fig. 5 illustrates the steady-state current-voltage relationships for oocytes before and ~15 min after IP_3 injection. The membrane was stepped from a holding potential of −35 to +20 mV for 1 s before stepping to different test potentials between −140 mV and +80 mV for 1 s. The current at the end of the test pulse was plotted vs. the test potential. Under basal conditions, the cell exhibited a small outwardly rectifying current with a slope conductance between 0 mV and −140 mV of ~3 μS (Fig. 5, *A* and *D*). 15 min after injection of IP_3 (Fig. 5 *B*), the cell exhibited a tilde (~)-shaped current voltage relationship: that is, the current negative to the reversal potential inwardly rectified and the current positive to the reversal potential outwardly rectified (Fig. 5 *D*). The current had a reversal potential near the calculated Cl equilib-

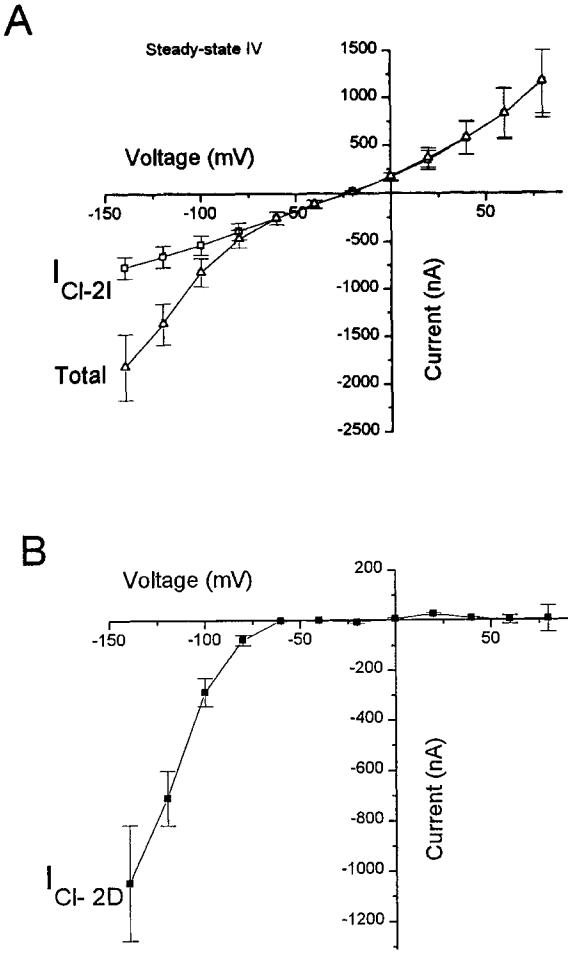

FIGURE 6. Steady-state IV relationships for the time-dependent and time-independent components of $I_{Cl\text{-}2}$. The voltage protocol shown in Fig. 5 was used. (*A*) Current-voltage relationships for total (*open triangles*) and time-independent (*open squares*) component of $I_{Cl\text{-}2}$. The total $I_{Cl\text{-}2}$ current was measured as the current at the end of the voltage pulse (1,995 ms) as shown in Fig. 5 *D* (*open circles*). The time-independent component was measured as the current at 1,020 ms. (*B*) Current-voltage relationship for the time-dependent component of $I_{Cl\text{-}2}$ The difference between the current at 1,995 and 1,020 ms was plotted as a function of the command potential.

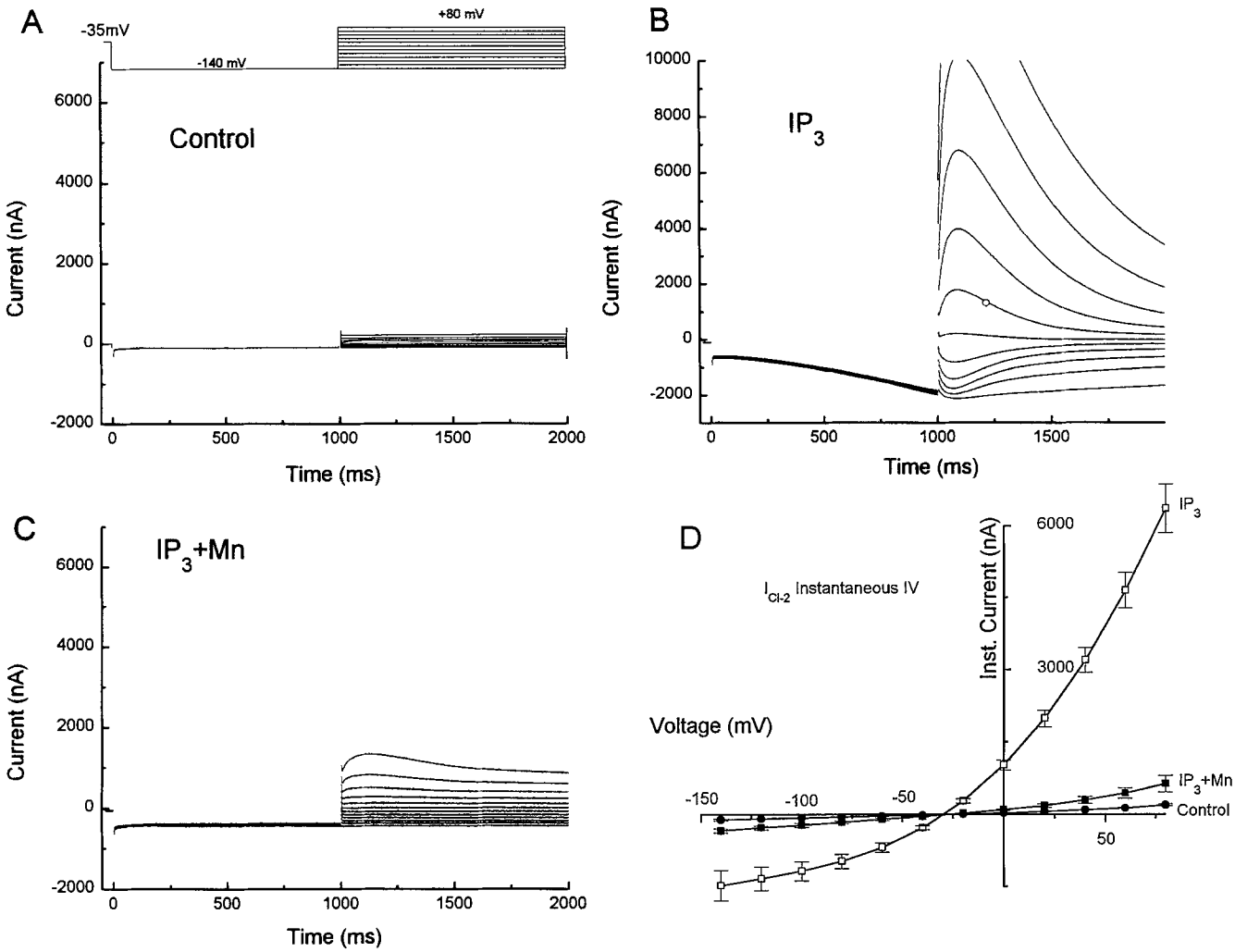

FIGURE 7. Instantaneous I-V relationship for $I_{Cl\text{-}2}$. Instantaneous IV relationship was determined by giving a 1-s duration pulse to −140 mV from a holding potential of −35 mV followed by a 1-s test pulse to different potentials. (*A*) IV traces before IP_3 injection. (*B*) IV traces ~15 min after IP_3 injection. (*C*) IV traces after IP_3 injection with 1 mM $MnCl_2$ added to the bath. (*D*) Average instantaneous current-voltage relationship for four oocytes determined as shown in *A–C*. The current 4 ms after stepping to the test potential (current at 1,004 ms) was plotted as a function of the test potential. Before IP_3 injection (*filled circles*), after IP_3 injection (*open squares*), and after IP_3 injection with 1 mM $MnCl_2$ in the bath (*filled squares*). The slowly developing current during the test pulse is described in more detail in Fig. 11.

rium potential. When 1 mM $MnCl_2$ was added to the bathing solution, the time-dependent component of $I_{Cl\text{-}2}$ was completely blocked. The time-independent current was partly reduced but usually remained larger than before IP_3 injection (Fig. 5, *C* and *D*). These results are consistent with the suggestion that the time-dependent component $I_{Cl\text{-}2}$ was a Cl current that required Ca influx to be activated.

$I_{Cl\text{-}2}$ consists of two components. The current that we have termed $I_{Cl\text{-}2}$ consisted of two components: a time-independent component and a time-dependent component. The current-voltage relationships of the time-dependent and time-independent components are plotted separately in Fig. 6. The time-independent component was measured as the current at 1,020 ms, and the time-dependent component was measured as the difference between the current at 1,995 ms and the current at 1,020 ms. The steady-state time-dependent component appeared to rectify inwardly, whereas the current-voltage relationship of the time-independent component was essentially linear. We term these two components $I_{Cl\text{-}2D}$ for time-dependent and $I_{Cl\text{-}2I}$ for time-independent components. As discussed below, we believe that $I_{Cl\text{-}2I}$ is actually $I_{Cl\text{-}1}$ because it exhibits properties we would predict from the characterization of $I_{Cl\text{-}1}$.

Instantaneous IV relationship. The steady-state IV curve in Fig. 6 showed that $I_{Cl\text{-}2D}$ inwardly rectified. To determine the cause of this rectification, we measured the instantaneous IV relationship and the activation curve for $I_{Cl\text{-}2}$ using tail current analysis. The instantaneous current-voltage relationships were determined before (Fig. 7 *A*) and ~15 min after (Fig. 7 *B*) injecting IP_3. In

this experiment, the membrane was hyperpolarized to −140 mV to activate $I_{Cl\text{-}2}$ and then repolarized to different test potentials. During the test pulse, an outward current developed with time. This current will be described in more detail in Fig. 11, but in the present experiment the instantaneous current was measured 4 ms after the test step. The instantaneous current at the test potential reflected the current through the channels that were open at −140 mV, before any channels had time to open or close. The basal current-voltage relationship slightly outwardly rectified and reversed at −25 mV, suggesting the presence of a small basal Cl current. After injection of IP_3, the current increased at least 10-fold (Fig. 7 *D*). The current-voltage relationship strongly outwardly rectified and reversed at the Cl equilibrium potential. The time-dependent component of $I_{Cl\text{-}2}$ was completely blocked by 1 mM Mn (Fig. 7 *C*). It was also blocked by 0.5 mM niflumic acid.

In the experiment of Fig. 7, we did not differentiate between $I_{Cl\text{-}2D}$ and $I_{Cl\text{-}2I}$ To determine the instantaneous IV relationship of $I_{Cl\text{-}2D}$ the IV curve of the time independent component (Fig. 6 *A*, *squares*) was subtracted from the IV curve of the total $I_{Cl\text{-}2}$ current (Fig. 7 *D*, *squares*). Fig. 8 *A* shows these curves, and Fig. 8 *B* shows the subtracted IV relationship. The IV relationship of $I_{Cl\text{-}2}$ strongly outwardly rectified. This seemed paradoxical, because the steady-state IV inwardly rectified. To resolve this paradox, we determined its activation curve.

Activation curve. The activation curve for $I_{Cl\text{-}2}$ is shown in Fig. 9. The activation curve for $I_{Cl\text{-}2}$ was determined by hyperpolarizing to different pre-potentials to activate $I_{Cl\text{-}2}$ and then repolarizing to +20 mV to measure the instantaneous outward current through the channels that were open at the end of the prepulse. Fig. 9 *A* shows a typical activation protocol, and Fig. 9 *B* shows the average activation curve for five oocytes. $I_{Cl\text{-}2}$ began to activate at potentials negative to −30 mV and exhibited a half-activation potential of −105 mV. At potentials negative to −150 mV, there was typically a decrease in $I_{Cl\text{-}2}$ relative to the current at −140 mV. The activation curve in Fig. 9 *B* shows that the steady-state IV curve in Fig. 8 inwardly rectified because the channel did not activate at potentials positive to −30 mV. Different batches of oocytes exhibited some variability in the half-activation potential (±10 mV). The reasons for this variability have not been investigated further.

$I_{Cl\text{-}1}$ and $I_{Cl\text{-}2}$ Are Ca Activated

We hypothesize that $I_{Cl\text{-}1}$ is a Ca-activated Cl current that is induced by Ca released from intracellular stores and that $I_{Cl\text{-}2D}$ is a Ca-activated Cl current that is induced by Ca influx from the extracellular space. As a test of the hypothesis that these currents were Ca-activated, we first injected the oocyte with 46 nl of 100 mM K_4-BAPTA followed ~5 min later by an injection of 23 nl of 10 mM IP_3. In oocytes that had been injected with BAPTA, injection of IP_3 failed to induce any currents (Fig. 10 *A*), whereas in control oocytes, IP_3 injection evoked both $I_{Cl\text{-}1}$ and $I_{Cl\text{-}2}$ in 95% of the oocytes.

We also examined the ability of BAPTA to block $I_{Cl\text{-}2}$ after it had already developed in response to IP_3 injection. Injection of BAPTA 10 min after IP_3 injection had fully activated $I_{Cl\text{-}2}$ invariably blocked the time-dependent component $I_{Cl\text{-}2D}$ (Fig. 10 *B*). In this example, the

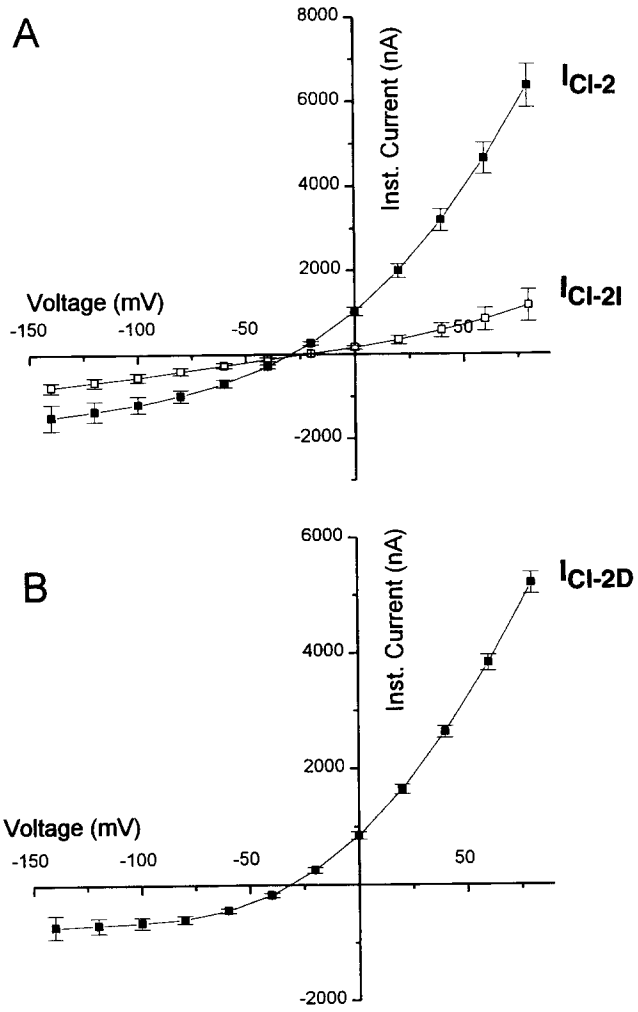

FIGURE 8. Instantaneous IV relationship for the time-independent and time-dependent components of $I_{Cl\text{-}2}$. To determine the instantaneous IV relationship of $I_{Cl\text{-}2D}$ the IV curve of the time independent component (Fig. 6 *A*, *open squares*) was subtracted from the IV curve of the total $I_{Cl\text{-}2}$ current (Fig. 7 *D*, *open squares*). (*A*) Time-independent component of $I_{Cl\text{-}2}$ (*open squares*) from Fig. 6 *A* and the instantaneous IV relationship of the total $I_{Cl\text{-}2}$ (*solid squares*) from Fig. 8 *A*. (*B*) Subtraction of the two curves in *A* gives the instantaneous IV relationship for the time-dependent component of $I_{Cl\text{-}2}$ shows these curves, and *B* shows the subtracted IV relationship.

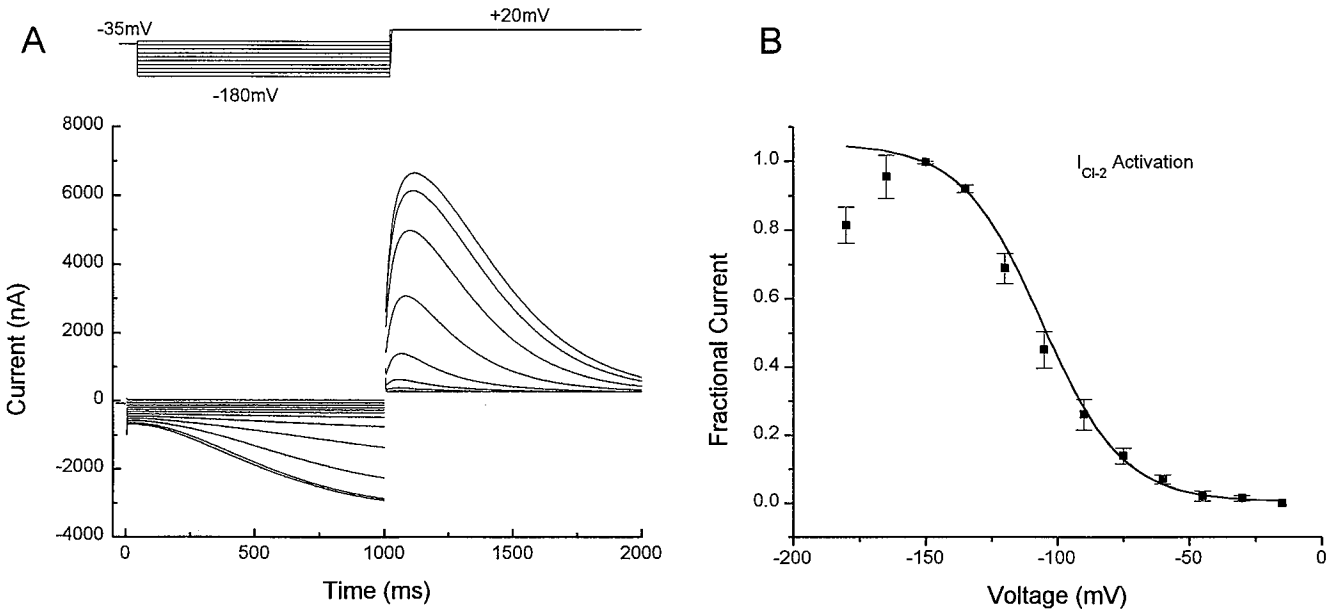

FIGURE 9. Activation curve of I_{Cl-2}. The activation curve was determined by stepping the membrane to different prepotentials between −160 and −20 mV for 1-s from a holding potential of −35 mV and then stepping to a test potential of +20 mV for 1-s. (*A*) Traces showing the determination of the activation curve. (*B*) The current 4-ms after stepping to the test potential was plotted as a function of the prepotential. The current for each oocyte was normalized so that the current after the −150 mV prepulse was set to 1.0. The data between −150 and −20 mV were fitted by the Boltzmann equation: $I = 1.05/[1 + \exp^{(V - 105)/15}]$.

time-independent component I_{Cl-2I} was apparently not blocked, but this conclusion is complicated by the fact that BAPTA alone often produced an increase in inward current that we have not fully characterized.

To determine the source of the Ca responsible for activation of I_{Cl-2D}, we bathed the cell in solution in which the $CaCl_2$ was replaced with $BaCl_2$ (Fig. 10, *C* and *D*). Under these conditions, injection of IP_3 still activated I_{Cl-1}, but I_{Cl-2D} was not activated. There was an increase in inward current at −120 mV that corresponded to I_{Cl-2I}. Similar results were observed when 1 mM Mn or La was added to the normal Ca-containing solution. Furthermore, addition of Mn (Fig. 7 *C*) or removal of Ca blocked I_{Cl-2D} (see Fig. 13). These results are consistent with the hypothesis that Ca influx is required for activation of I_{Cl-2D}. Our interpretation is that IP_3 first stimulates Ca release from internal stores which activates I_{Cl-1}. The "depletion" of Ca from stores then activates capacitative Ca entry which is responsible for I_{Cl-2D} activation.

Activation of I_{Cl-1} by Ca Influx

We believe that the kinetics of decline of I_{Cl-1} at +20 mV in Fig. 1 reflects the time course of depletion of Ca stores. Fig. 1 *B* may give the additional impression that I_{Cl-1} cannot be activated in response to Ca influx, because I_{Cl-1} declines (almost) to baseline within ~3 min after IP_3 injection. However, this impression is incorrect. Because the steady-state current voltage relationship of I_{Cl-1} outwardly rectifies, whereas Ca influx will be greatest at hyperpolarized potentials, one would expect steady-state I_{Cl-1} to be small at all potentials after stores are depleted. If this reasoning is correct, we should be able to reactivate I_{Cl-1} after Ca stores are depleted by first giving hyperpolarizing pulses to increase Ca influx followed by depolarizations to activate the Cl channels. To test this hypothesis, we performed the test shown in Fig. 11. In this experiment, the oocyte was injected with IP_3 while stimulating with a voltage protocol similar to, but different from, the protocol used in Fig. 1. In this protocol the membrane was first stepped to −120 mV and then to +20 mV. The rationale was that Ca entering the cell when the driving force for Ca entry was high at −120 mV could activate I_{Cl-1} at +20 mV, a potential which would open the voltage gates for I_{Cl-1}. Fig. 11 *A–F* shows the currents 40 s before and 40, 50, 100, 150, and 350 s after injecting IP_3. At ~40 s after IP_3 injection, I_{Cl-1} was activated exactly as described in Fig. 1. However, as I_{Cl-1} declined, it was replaced with an outward current exhibiting a different waveform that grew in amplitude in concert with the development of I_{Cl-2}. The time course of development of these currents is shown in Fig. 11 *H*, where the circles show the initial development of I_{Cl-1} measured at the end of the +20 mV pulse, the squares show the development of I_{Cl-2} at the end of the −120 mV pulse, and the triangles show the current at 85 ms after the step to +20 mV. The inactivating outward current at +20 mV which peaks in ~85 ms is referred to as I_3.

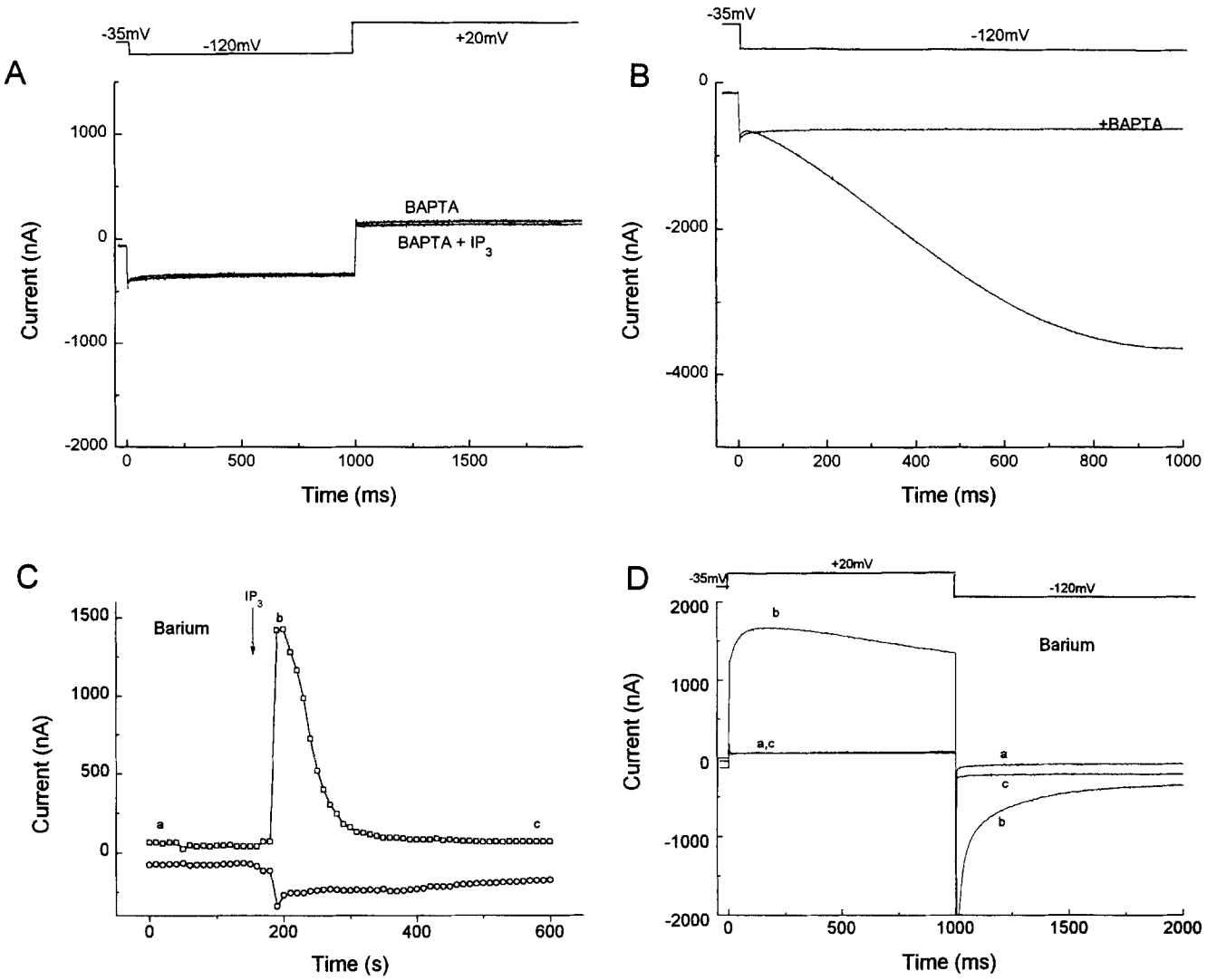

FIGURE 10. Effect of Ba and BAPTA on the stimulation of $I_{Cl\text{-}1}$ and $I_{Cl\text{-}2}$. (*A*) The oocyte was first injected with 23 nl 50 mM K_4·BAPTA. This injection usually produced an increase in time-independent inward current. 5 min later, 23 nl of 10 mM IP_3 was injected. The superimposed traces shown were taken 5 min after BAPTA injection and 15 min after IP_3 injection. IP_3 fails to stimulate $I_{Cl\text{-}1}$ or $I_{Cl\text{-}2}$. (*B*) Effect of BAPTA injection on $I_{Cl\text{-}2}$. The cell was first injected with 4.6 nl 10 mM IP_3. The first trace shown was taken 15 min after IP_3 injection. Subsequently, 23 nl of 50 mM BAPTA was injected. The BAPTA trace was taken 5 min after BAPTA injection. The time-dependent component of $I_{Cl\text{-}2}$ is completely blocked. (*C*) Effect of extracellular Ba on stimulation of $I_{Cl\text{-}1}$ and $I_{Cl\text{-}2}$. The $CaCl_2$ in the extracellular solution was replaced with 2 mM $BaCl_2$. At the time indicated, 4.6 nl 10 mM IP_3 was injected while the cell was stimulated with a 1-s pulse to +20 mV followed by a 1-s pulse to −120 mV from a holding potential of −35 mV. *Open squares*, current at the end of the +20 mV pulse ($I_{Cl\text{-}1}$); *open circles*, current at the end of the −120 mV pulse ($I_{Cl\text{-}2}$). (*D*) Current traces from the same experiment as in *C*. The traces *a* (before IP_3), *b* (20 s after IP_3), and *c* (400 s after IP_3) correspond to the times indicated in *C*.

The inactivating outward current at +20 mV has characteristics of $I_{Cl\text{-}1}$. We hypothesize that the inactivating outward current at +20 mV (I_3) in this protocol is $I_{Cl\text{-}1}$ because its instantaneous current-voltage relationship resembles $I_{Cl\text{-}1}$ and because it activates with a time constant virtually identical to $I_{Cl\text{-}1}$. These features are illustrated in Fig. 12. The instantaneous IV relationship of the inactivating outward current was determined in an oocyte previously injected with IP_3 by stepping the membrane to −120 mV for 1 s to produce Ca influx, followed by a step to +80 mV for 50 ms to activate the outward current and then stepping to different potentials for measuring the instantaneous current (Fig. 12 *A*). Fig. 12 *A* begins with the +80 mV pulse. The traces shown were obtained by subtracting the currents before injecting IP_3 from those after injecting IP_3, thus the IV relationship reflects only IP_3-activated current. Identical results were also obtained by subtracting currents in the absence and presence of Ca in the bath. The instantaneous IV relationship was nearly linear (Fig. 12 *B*), which is very similar to the IV relationship of $I_{Cl\text{-}1}$ (Fig. 3 *C*). The small outward rectification could possibly be

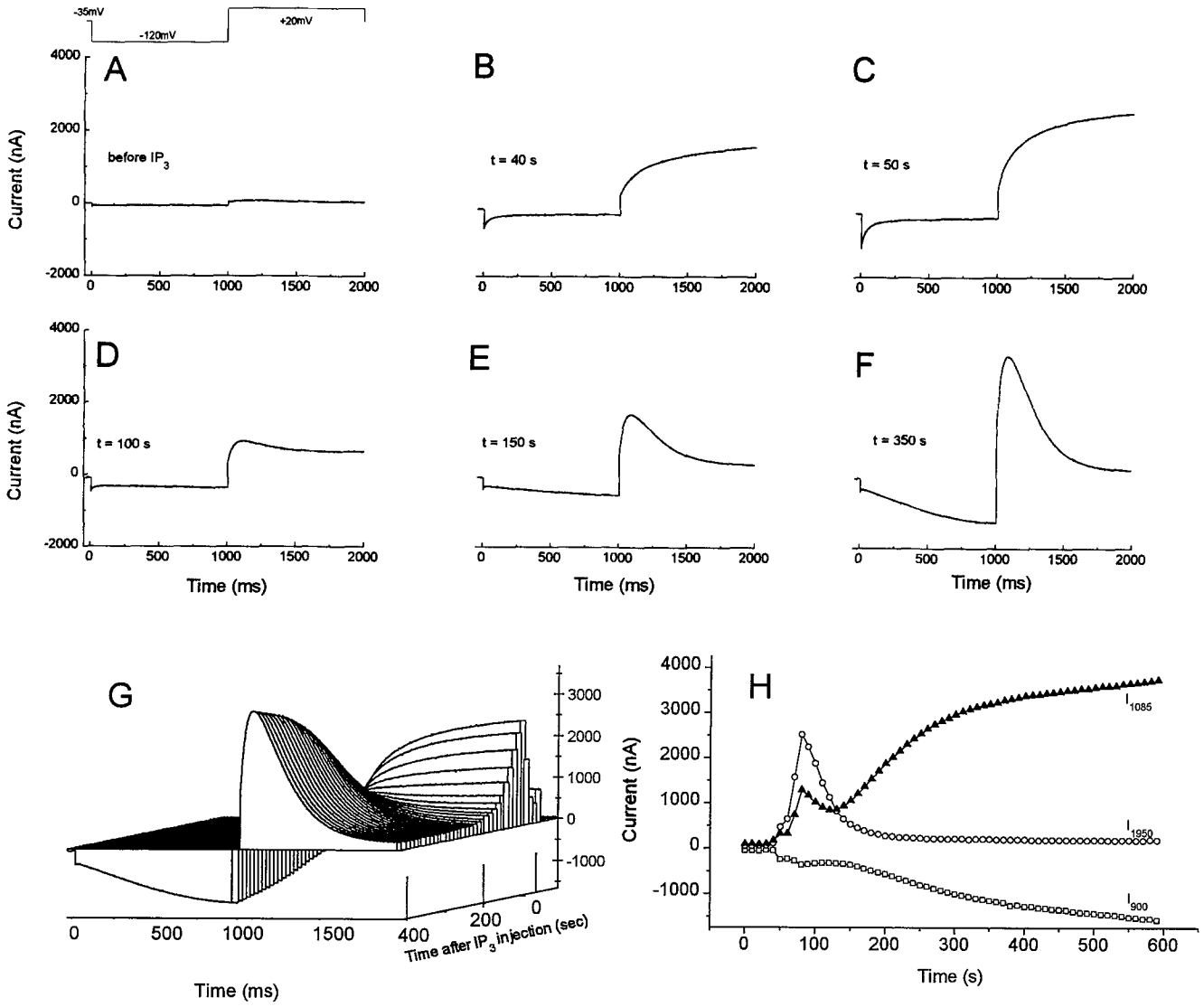

FIGURE 11. An inactivating time-dependent outward current (I_3) develops slowly after IP_3 injection. The experimental design is similar to that in Fig. 1, except that the voltage protocol was reversed: a 1-s pulse to −120 mV was followed by a pulse to +20 mV from a holding potential of −35 mV. *A–F* show current traces before and at various times after IP_3 injection. Note the change with time of the kinetics of the outward current at +20 mV. At t = 50s (*C*) the current does not inactivate. It then declines in amplitude (*D*) and is replaced by an inactivating outward current (*F*) that grows in amplitude concurrently with the development of $I_{Cl\text{-}2}$. (*G*) Another way of displaying the data of *A–F* to give a more dynamic view of the change in the outward current. 40 traces are stacked together in the z-axis starting with the first trace at the back and ending with the trace at 400 s after IP_3 injection at the front. The x-axis is the time of the 2-s voltage pulse and the y-axis is the amplitude. (*H*) The time course of change in currents after IP_3 injection. *Open circles*, $I_{Cl\text{-}1}$ measured as the current near the end of the +20 mV pulse (1,950 ms); *open squares*, $I_{Cl\text{-}2}$ measured as the current near the end of the −120 mV pulse (900 ms); *filled triangles*, peak of the transient outward current (I_3), measured as the current at 1,085 ms.

due to contamination of this current with $I_{Cl\text{-}2}$ which may not completely deactivate during the 50 ms pulse to +80 mV. We have not succeeded in selectively blocking $I_{Cl\text{-}1}$ or $I_{Cl\text{-}2}$ so it has been impossible to evaluate the contamination of this outward current with the underlying deactivation of $I_{Cl\text{-}2}$. However, the IV curve is markedly different from that of $I_{Cl\text{-}2}$, suggesting that contamination is small.

The inactivating outward current activates with the same kinetics as $I_{Cl\text{-}1}$. With the voltage pulse to +20 mV, the inactivating outward current activated with a single exponential having τ = 25 ms (Fig. 12 *D*), which is very similar to the τ of the fast component of the activation of $I_{Cl\text{-}1}$ (Fig. 12 *C*). The decline of the current occurred with a τ = ~250 ms, which we presume is the time constant of reduction of cytosolic Ca upon depolarization.

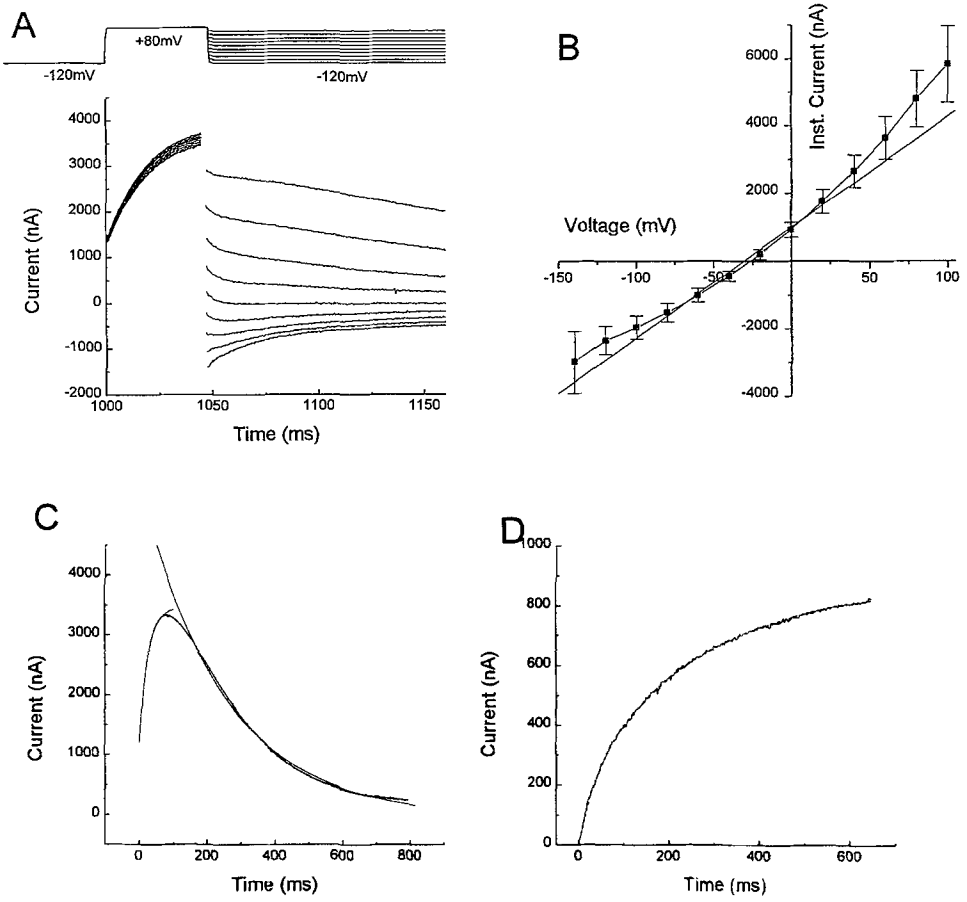

FIGURE 12. Instantaneous current-voltage relationship and kinetics of I_3 suggests it is probably $I_{Cl\text{-}1}$. (*A*) Instantaneous IV of I_3. The oocyte was stepped to −120 mV for 1-s before the start of the trace shown. The membrane was then stepped to +80 mV for 50-ms followed by steps to different test potentials. (*B*) The amplitude of the current 4 ms after stepping to the test potential was plotted vs. the test potential. The data are the averages of six oocytes. The straight line is drawn to indicate a linear IV relationship for a Cl conductance. (*C*) Kinetics of activation and deactivation of I_3. The outward current was activated by a pulse to +20 mV after a 1-s prepulse to −120 mV. The activation (0–100 ms) was fitted to a single exponential with a τ = 25 ms. The deactivation (200–800 ms) was fitted by a single exponential with τ = 246 ms. The thin lines show the fits and the noisy trace is the data. (*D*) Kinetics of activation of $I_{Cl\text{-}1}$. $I_{Cl\text{-}1}$ was activated by IP_3 injection and voltage steps from −35 to +20 mV. The onset of $I_{Cl\text{-}1}$ is fit to the sum of two exponentials with τ = 28 and 274 ms. The fit is the dashed line, which is very difficult to distinguish from the noisy data trace.

Effects of Extracellular Ca

"Capacitative Ca entry" is classically demonstrated by depleting intracellular Ca stores (with IP_3 or thapsigargin) in the absence of extracellular Ca and then measuring the current that is stimulated by addition of extracellular Ca. If $I_{Cl\text{-}2}$ is activated by Ca influx, we would expect it to be activated upon re-addition of Ca to the bath after injection of IP_3 in Ca-free solutions. Fig. 13 shows the effect of switching from 0-Ca Ringer to 2 mM Ca Ringer approximately 10 min after injection of IP_3. The cell was voltage clamped at −60 mV, and the holding current was measured. Switching from 0 to 2 mM Ca in oocytes that had not been injected with IP_3 usually produced no change in the holding current at −60 mV. However, as shown in Fig. 13, when the oocyte had previously been injected with IP_3, addition of Ca produced a rapid increase in inward current. The current reached a peak of −1,000 nA in several seconds and then rapidly declined to a plateau level of −250 nA, where it remained at least 10 min. To determine which currents were responsible for this inward current at −60 mV, we returned the oocyte to 0-Ca Ringer and then ran our standard voltage protocol: a 1-s pulse to −120 mV followed by a 1-s pulse to +20 mV from a holding potential of −35 mV. Fig. 13 *B–E* shows the current traces before and at different times after re-addition of 2 mM Ca. At 6 s after addition of Ca, a large $I_{Cl\text{-}2D}$ current was recorded at −120 mV followed by $I_{Cl\text{-}1}$ at +20 mV. Both $I_{Cl\text{-}2D}$ and $I_{Cl\text{-}1}$ increased transiently after addition of Ca and then declined to a lower plateau that remained relatively constant during the remainder of the recording. The time course of change of the currents (Fig. 13 *F*) closely approximated the time course of decline of the holding current at −60 mV (Fig. 13 *A*). The decline in current is presumably due to partial refilling of the Ca store by Ca influx.

Putative Store-operated Ca Current in Oocytes

Our interpretation of the data above presumes that there is a store-operated Ca current in oocytes. We have attempted to measure this current directly as shown in Fig. 14. In this experiment, we first injected IP_3 to release Ca from intracellular pools and then injected BAPTA to inhibit Ca-activated Cl currents. The cell was

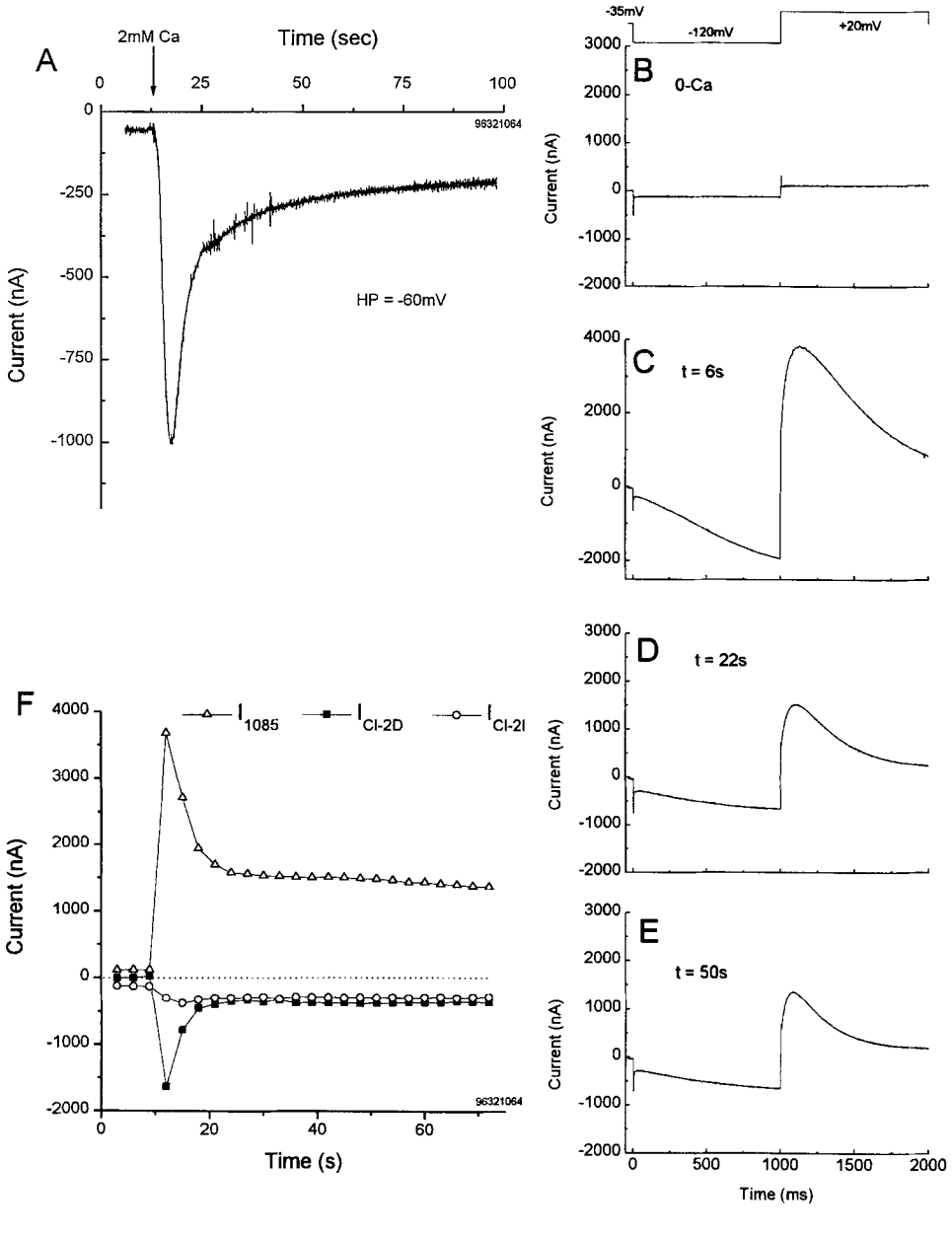

FIGURE 13. Effect of changing extracellular Ca on oocyte currents. The oocyte was injected with IP_3 with the oocyte bathed in normal Ringer about 10 min before the beginning of the recordings shown. After the development of I_{Cl-2} the oocyte was shifted into 0 Ca Ringer for ~2 min. (*A*) Effect of re-addition of 2 mM Ca to an oocyte bathed in 0-Ca Ringer after IP_3 injection. The membrane potential was held at −60 mV. The same oocyte was then shifted back to 0-Ca Ringer for ~2 min and the standard −120 to +20 mV voltage protocol (Fig. 11) was applied once every 3 s. (*B*) A sample current trace in response to the −120 to 20 mV protocol in 0-Ca Ringer. (*C–E*) Current traces recorded 6, 22, and 50 s after addition of 2 mM Ca to the bath. (*F*) Plot of the change in currents with time after adding 2 mM Ca. *Filled squares*, time-dependent component of I_{Cl-2}; *open circles*, time-independent component of I_{Cl-2}; *open triangles*, peak transient outward I_3 current at +20 mV (measured at 1,085 ms).

stimulated with 2-s duration ramp pulses from −160 to 50 mV. Under these conditions, shifting from 0-Ca to 10 mM Ca produced a shift in the ramp current (Fig. 14A). The difference in the ramp currents in the absence and presence of Ca (Fig. 14 *B*) resembles the store-operated Ca current I_{crac} in T-lymphocytes and mast cells (Hoth and Penner, 1993; Zweifach and Lewis, 1993; Premack et al., 1994). We cannot rule out the possibility that the difference current is residual Ca-activated Cl current not blocked by BAPTA, but the fact that there is no outward current at +50 mV (Fig. 14 *B*) argues against this possibility. The current is blocked by La, and its amplitude is related to the extracellular [Ca] and requires prior stimulation with IP_3 to be observed. Furthermore, this current activates in a voltage range that explains the activation of I_{Cl-2}

DISCUSSION

Conclusions

Xenopus oocytes exhibit two different Ca-activated Cl currents. In these studies we have shown that injection of IP_3 into *Xenopus* oocytes activates two different Ca-activated Cl currents. I_{Cl-1} is stimulated rapidly (within 5 s after IP_3 injection), exhibits time-dependent activation upon depolarization, a linear instantaneous IV relationship with a reversal potential near E_{Cl}, and a curvi-

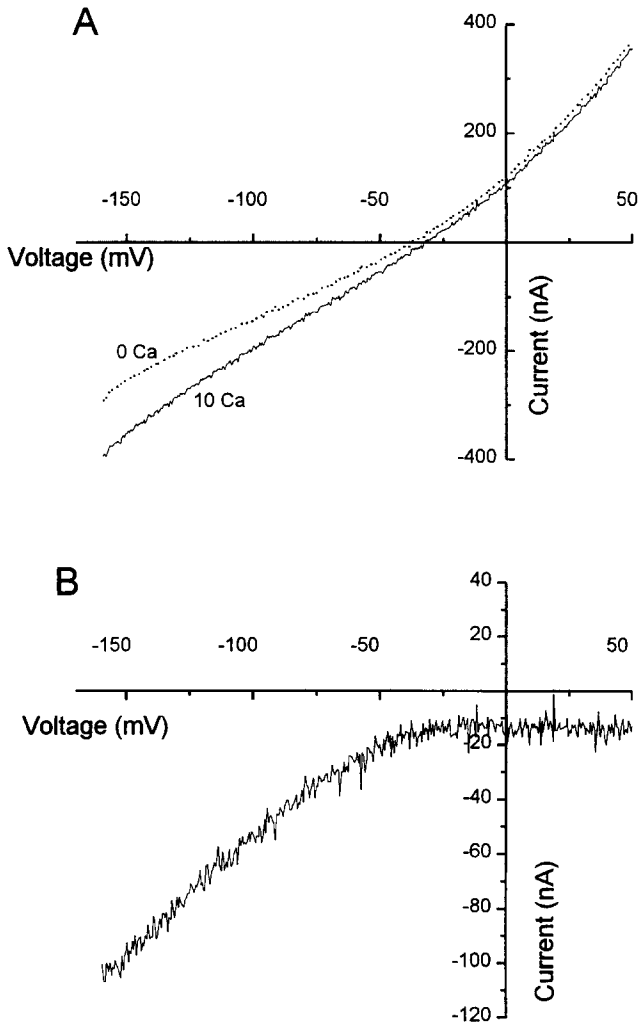

FIGURE 14. Putative store-operated Ca current in oocytes. The oocyte was injected with IP_3 ~15 min and with BAPTA ~10 min before the records shown here. The oocyte was placed in 0-Ca Ringer for 2 min, and the current recorded in response to a 2-s duration ramp pulse from −160 to +50 mV. The oocyte was shifted to 10 mM Ca and the current in response to the same ramp was recorded. The difference between these two currents (*bottom*) is the presumed store-operated Ca influx.

linear activation curve with an approximate half-maximal activation voltage of >200 mV. $I_{Cl\text{-}2}$ appeared to be composed of two components. The time-dependent component $I_{Cl\text{-}2D}$ is stimulated slowly after IP_3 injection (half-maximal stimulation occurs ~3 min after injection). $I_{Cl\text{-}2D}$ has a strongly outwardly rectifying instantaneous IV relationship with a reversal potential near E_{Cl} and is activated by hyperpolarization with a half-maximal activation voltage of −105 mV. The time-independent component $I_{Cl\text{-}2I}$ has a linear current-voltage relationship and a reversal potential near E_{Cl} and, as discussed below, is actually $I_{Cl\text{-}1}$.

$I_{Cl\text{-}1}$ is stimulated both by Ca released from stores and by Ca influx. We conclude that $I_{Cl\text{-}1}$ is stimulated by Ca released from pools for the following reasons: (*a*) Intracellular injection of IP_3 rapidly stimulates $I_{Cl\text{-}1}$, and the stimulation is blocked by intracellular injection of BAPTA. This suggests that $I_{Cl\text{-}1}$ is stimulated by Ca and not by IP_3 directly. (*b*) Injection of IP_3 stimulates $I_{Cl\text{-}1}$ even when Ba or Mn replace extracellular Ca, suggesting that the source of stimulating Ca is not Ca influx but rather release of Ca from stores. In our analysis of the properties of $I_{Cl\text{-}1}$ in Figs. 2–4, we presume that $[Ca]_i$ at short times after IP_3 injection is relatively independent of membrane potential because Ca influx through store-operated channels has not yet been activated. Furthermore, the voltage steps used to determine the activation curve were very brief and currents were measured 4 ms after the voltage steps. One would not expect cytosolic Ca to change significantly on this time scale. Thus, the curvilinear activation curve of $I_{Cl\text{-}1}$ reflects voltage-dependent gating of the channel and not the level of cytosolic free Ca.

In addition to actitvation by store Ca, $I_{Cl\text{-}1}$ can be stimulated by Ca influx after the stores have been depleted, provided that Ca influx is augmented by increasing the driving force for Ca entry by hyperpolarization immediately before voltage-dependent activation of $I_{Cl\text{-}1}$ by a depolarization. The slowly activating current upon stepping to +20 mV from −140 mV after IP_3 injection is $I_{Cl\text{-}1}$. There are several reasons why we believe that the inactivating outward current that develops with time after IP_3 injection upon depolarization to +20 mV from −140 mV (Fig. 11) is $I_{Cl\text{-}1}$: (*a*) The instantaneous current-voltage relationships of the inactivating outward current at +20 mV and $I_{Cl\text{-}1}$ are both linear. (*b*) Both currents activate with the same kinetics (τ = 25 ms). (*c*) The activation curve for $I_{Cl\text{-}1}$ predicts that more $I_{Cl\text{-}1}$ will activate with depolarizations to any potential positive to −140 mV (Fig. 4). In fact, Fig. 7 *B* shows that upon stepping from −140 mV to various potentials, inward currents are activated negative to E_{Cl} whereas outward currents are activated positive to E_{Cl}. This interpretation differs from that of Yao and Parker (1993) (see below).

The time-independent component of $I_{Cl\text{-}2}$ is probably $I_{Cl\text{-}1}$ for the following reasons: (*a*) One would expect an inward current through $I_{Cl\text{-}1}$ channels at potentials between E_{Cl} and −150 mV based on its activation curve (Fig. 4). (*b*) Both $I_{Cl\text{-}1}$ and $I_{Cl\text{-}2I}$ have a linear current-voltage relationship (Fig. 3 *C* and 8 *A*). (*c*) $I_{Cl\text{-}1}$ and $I_{Cl\text{-}2I}$ exhibit identical time courses in Ca-jump experiments (Figs. 13 and 14). The only experiment in possible conflict with this interpretation is that $I_{Cl\text{-}2I}$ was apparently not blocked by internal BAPTA (Fig. 10 *B*). However, this experiment may be misleading because injection of BAPTA itself before IP_3 produces an increase in inward

current. Thus, the apparent absence of effect of BAPTA on the time-independent inward current may be due to two opposite effects. $I_{Cl\text{-}2I}$ is completely blocked by 0-Ca extracellular solution (Fig. 13).

$I_{Cl\text{-}2D}$ is stimulated by Ca influx through store-operated Ca channels. We hypothesize that $I_{Cl\text{-}2D}$ is preferentially activated by Ca influx through store-operated Ca channels for the following reasons: (*a*) $I_{Cl\text{-}2D}$ requires Ca for activation, as it is blocked by intracellular injection of BAPTA. (*b*) $I_{Cl\text{-}2D}$ requires Ca influx for activation, because it is blocked by addition of Ba or Mn to the extracellular solution or removal of extracellular Ca. (*c*) The time course of stimulation of $I_{Cl\text{-}2D}$ corresponds with the time course of emptying intracellular Ca stores as assessed by the decline of $I_{Cl\text{-}1}$. (*d*) The time course of activation of $I_{Cl\text{-}2}$ upon stepping from −35 to −120 mV reflects the time course of accumulation of Ca in the cytosol as measured by the amplitude of $I_{Cl\text{-}1}$ on stepping to +20 mV at different times during the hyperpolarizing step (data not shown).

The Ca concentration-jump experiment of Fig. 13 provides additional insight into the regulation of $I_{Cl\text{-}2D}$. When the oocyte is shifted from 0-Ca to 2 mM Ca after IP_3 injection, the first hyperpolarization produces a large $I_{Cl\text{-}2}$. This declines rapidly to a steady-state level that is less than half the amplitude of the initial current. We presume that this decline reflects refilling of the Ca stores over this ~15-s period and a subsequent decrease in Ca influx. When the oocyte is shifted to 10 mM Ca (data not shown), the initial $I_{Cl\text{-}2}$ is extremely large, but it declines even more rapidly than with 2 mM Ca and quickly disappears. However, even though $I_{Cl\text{-}2}$ has disappeared, $I_{Cl\text{-}1}$ remains very large. There are several possible explanations of this result. One possibility is that the Ca influx refills the Ca stores, and the store-operated Ca channels subsequently close completely, but $I_{Cl\text{-}1}$ remains elevated because of oscillatory Ca release from stores.

Store-operated Ca current. The activation of $I_{Cl\text{-}2}$ by hyperpolarizing steps (Fig. 9) in principle could be explained either by strictly voltage-dependent gating of the Cl channels or could result indirectly from the voltage-dependent influx and accumulation of Ca. The latter possibility seems more likely because the putative store-operated Ca current (Fig. 14) predicts the activation of $I_{Cl\text{-}2}$. That is, the store-operated current activates significantly only at potentials negative to −50 mV, as does $I_{Cl\text{-}2}$. This current-voltage relationship for the store-operated Ca influx explains why the inactivating outward $I_{Cl\text{-}1}$ current is present only when the membrane is hyperpolarized to potentials negative to −50 mV before the depolarizing step (Fig. 9 *A*). The observation that the voltage range for activation of outward $I_{Cl\text{-}1}$ parallels the activation range for the putative store-operated current (Fig. 14) provides an additional argument that this current is a store-operated current. The other arguments are that this current is dependent on extracellular Ca, is blocked by La, and is present when all Ca-activated Cl currents measured by our conventional protocols are blocked by intracellular BAPTA.

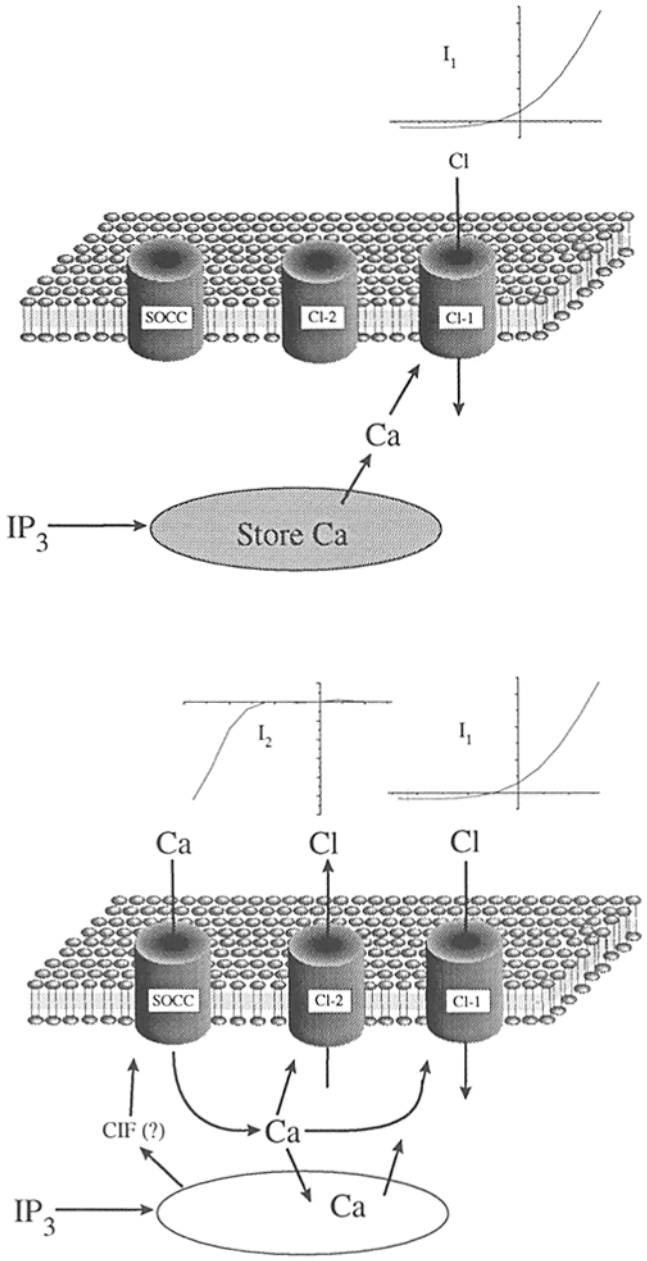

FIGURE 15. Model of regulation of Cl channels in *Xenopus* oocytes. (*Top*) When the oocyte is injected with IP_3, Ca is mobilized from stores and $I_{Cl\text{-}1}$ is induced. The steady-state current-voltage relationship of $I_{Cl\text{-}1}$ is shown above. (*Bottom*) After some minutes, depletion of the store triggers opening of store-operated Ca channels (possibly via a calcium influx factor, *CIF*). Ca influx then induces both $I_{Cl\text{-}1}$ and $I_{Cl\text{-}2}$. The steady-state current voltage relationships are shown above to indicate that the currents that flow depend upon potential. Ca influx may also serve to replenish the pool.

Model of regulation of Ca-activated Cl channels in Xenopus oocytes. Our model for regulation of Cl channels by Ca is shown in Fig. 15. Injection of IP_3 stimulates release of Ca from stores, which rapidly stimulates $I_{Cl\text{-}1}$ channels (upper panel). As the stores become depleted, store-operated Ca channels are activated which can stimulate both $I_{Cl\text{-}1}$ and $I_{Cl\text{-}2}$ depending on potential (lower panel). It should be noted that because we have not inhibited the Ca-ATPase, Ca uptake into the SR has not been inhibited. Thus, activation of $I_{Cl\text{-}1}$ at long times after IP_3 injection could actually be due to Ca entering the cell via influx subsequently entering Ca stores and subsequently activating $I_{Cl\text{-}1}$.

At present we have no explanation why store Ca is not capable of activating $I_{Cl\text{-}2}$. It seems unlikely that the explanation is that $I_{Cl\text{-}1}$ and $I_{Cl\text{-}2}$ have different sensitivities to Ca. Approximately the same amount of $I_{Cl\text{-}1}$ is activated by store Ca and by Ca influx (Fig. 11). If we assume that the amplitude of $I_{Cl\text{-}1}$ is a relative measure of the amount of Ca near these channels, this suggests that approximately the same amount of Ca is present at the membrane under these two conditions. Thus, it seems that spatial and temporal aspects of Ca concentration must be important (Lechleiter and Clapham, 1992).

Voltage-gated Ca Current

The above conclusions could be compromised if Ca influx through voltage-gated Ca channels was partly responsible for activation of these Cl currents. *Xenopus* oocytes have been shown to have endogenous voltage-gated Ca channels (Dascal, 1987) that might be expected to contribute Ca influx to activate Cl currents. Such a Cl current ($I_{Cl(Ca)}$) activated by Ca influx through voltage-gated channels has been described by Barish (1983) and Miledi (1982). However, there are a number of reasons why Ca influx via voltage-gated channels is unlikely to contribute significantly to the currents described here. (*a*) $I_{Cl(Ca)}$ described by Barish (1983) is at least 10-times smaller than the currents we have described here with physiological concentrations of external Ca. (*b*) The IV relationship for $I_{Cl(Ca)}$ is ∩-shaped with a peak near 0 mV, reflecting the IV relationship of the voltage-gated Ca channels (Barish, 1983). Neither $I_{Cl\text{-}1}$ nor $I_{Cl\text{-}2}$ exhibit an obvious component with this shape IV relationship. (*c*) In the experiments on $I_{Cl\text{-}1}$ in Figs. 2–4, $I_{Cl\text{-}1}$ did not require extracellular Ca. Furthermore, the holding potential was −35 mV which would largely inactivate the voltage-gated Ca channels (Dascal et al., 1986). Thus, the properties of $I_{Cl\text{-}1}$ activated by store Ca would not be convoluted by any contribution from $I_{Cl(Ca)}$. (*d*) In principle, Ca influx via voltage-gated Ca channels could possibly confound the tail analysis of $I_{Cl\text{-}2}$, if the test depolarizations after the −120 mV steps (Fig. 7) were to activate voltage-gated Ca channels (that could not be resolved from the capacitative transient) with the resulting Ca influx activating Cl channels. In fact, however, the contribution of Ca influx via voltage-gated channels is not important because the envelope-of-tails test (Hodgkin and Huxley, 1952) shows that the tail currents precisely predict the time course of $I_{Cl\text{-}2}$, which would not be true if a voltage-gated Ca influx were contributing to currents recorded during the tail. Furthermore, neither 100 μM nickel nor 10 μM nifedipine, which block the endogenous T-like and L-like Ca currents in the oocyte (Barish, 1983; Dascal et al., 1986; Dascal, 1987), had any effect on the shape of the $I_{Cl\text{-}2}$ IV relationship, although they both decreased the amplitude of $I_{Cl\text{-}2}$ ~50%.

Relationship to Other Studies

Since the early 1980's, a great deal has been learned about Ca signaling and Cl channels in *Xenopus* oocytes largely as the result of the pioneering work of R. Miledi and I. Parker, Y. Lass and N. Dascal, and M. Berridge and R.F. Irvine and their colleagues. The ionic currents that we have described here have been observed by these investigators previously. However, the present study adds to the earlier ones by characterizing the biophysical properties of these channels in more detail to show that there are clearly two different kinds of Ca-activated Cl channels that are regulated differently.

IP_3 activates Cl currents with several components. In reading the literature on *Xenopus* oocytes, one can divide Cl current responses to agents that mobilize store Ca into three different groups based on their time courses and dependence on extracellular Ca. The first response is a transient current that activates and inactivates in ~2 min and is not dependent on extracellular Ca. This current is very similar to $I_{Cl\text{-}1}$ and is likely to be caused by release of Ca from stores by IP_3. The second component is also independent of extracellular Ca, but develops slowly after release of store Ca. This current may be activated by a slower mobilization of store Ca under certain conditions and may also be mediated by $I_{Cl\text{-}1}$. The third component is identical to $I_{Cl\text{-}2}$ in that it is activated at hyperpolarizing potentials and requires extracellular Ca. Despite the fact that it is possible to identify these three kinds of responses based on time course and sensitivity to Ca_o, it is difficult to compare results of different investigators unambiguously, because the current responses in the various studies were often not characterized in sufficient detail either biophysically or pharmacologically. For example, current voltage relationships of currents that one might expect to be the same based on their time course and Ca_o sensitivity are often different.

Most publications have focussed on only one or two of these components, but all three components were observed in the same oocytes by Snyder et al. (1988),

who demonstrated that IP_3 injection into the oocyte induced an inward current at −50 mV holding potential having three components. One component called I_{1a} was independent of Ca influx and activated and inactivated in ~2 min. I_{1b} was also independent of Ca influx, but activated much more slowly and lasted ~10 min or more. I_2 was dependent on Ca influx and activated slowly. It would seem that the fast Ca-influx independent component corresponds to our $I_{Cl\text{-}1}$ and the slow Ca-influx dependent component corresponds to our $I_{Cl\text{-}2}$ but the biophysical properties of these currents were not determined (Snyder et al., 1988). Other studies usually describe two components, but the dependence of the components on Ca influx is rather variable.

In some studies, IP_3 injection or activation of receptors that activate phospholipase C induced two Ca-dependent Cl currents that did not require Ca influx. In response to IP_3 injection, a transient current developed rapidly upon IP_3 injection and this was often followed by a more slowly developing component that was frequently oscillatory in nature (Oron et al., 1985; Parker and Miledi, 1986; Berridge, 1988; Parker and Ivorra, 1991). The amplitude of the second component seemed to be quite variable in amplitude from oocyte to oocyte (Parker and Ivorra, 1991). Activation of muscarinic receptors also activated two consecutive inward Cl currents at −60 mV (D_1 and D_2 responses) that were mimicked by IP_3 injection and were independent of Ca_o (Oron et al., 1985; Gillo et al., 1987). There does not seem to be agreement about the shape of the IV relationships of the currents induced by IP_3 or receptor activation. The currents have been described as both weakly outwardly rectifying (Dascal et al., 1984; Oron et al., 1985) and very strongly outwardly rectifying (Miledi et al., 1989). A strongly rectifying Ca-activated Cl current is also induced by injection of Ca into oocytes (Miledi and Parker, 1984).

In other studies, however, IP_3 injection or activation of PLC-coupled receptors induced two Ca-activated Cl currents, but only the first component was independent of Ca_o (Parker et al., 1985; Parker and Miledi, 1987; Miledi et al., 1989; DeLisle et al., 1992; Lupu-Meiri et al., 1993; Petersen and Berridge, 1994). The second component which was called T_{in} and first described in detail by Parker et al. (1985) and Parker and Miledi (1987) requires Ca influx and is very likely the same as $I_{Cl\text{-}2}$ described here. Parker et al. (1985) demonstrated that in some, but not all, native oocytes hyperpolarization produced a small transient inward current that increased with hyperpolarization and had a duration of several seconds. These authors reported that this current was frequently labile and disappeared after several minutes. A similar but much larger current was found in oocytes expressing receptors coupled to phospholipase C when the receptors were activated by agonist. T_{in} is a Cl current with a steady-state current-voltage relationship that resembles $I_{Cl\text{-}2}$. The current is blocked by Mn-containing or 0-Ca extracellular solutions and is blocked by EGTA injection into the oocyte. This current is also activated in native oocytes by injection of IP_3. Petersen and Berridge (1994) have shown that LPA (via a PLC-coupled receptor), thapsigargin, and IP_3 activate currents that resemble $I_{Cl\text{-}1}$ and $I_{Cl\text{-}2}$ with regard to their differing dependence on Ca_o and time course. Indeed, Petersen and Berridge (1994) have presented data similar to our Fig. 13, but they seem to interpret the data in terms of a single Cl conductance rather than multiple conductances.

Stimulation of the serotonin (5-HT) (1C) receptor in oocytes also produced an initial rapid oscillatory current followed by a pronounced secondary current (Parekh et al., 1993), but separation of the two components into Ca_o-dependent and independent components was not as clear. The initial component was reduced ~35% by 0-Ca and thus may be partially dependent on Ca influx. The secondary component was blocked by 100 μM Cd and was sensitive to the concentration of extracellular Ca, suggesting that this component required Ca influx. In these same studies, injection of IP_3 produced variable responses: either an oscillatory current or a rapid current followed by a sustained secondary one. The sustained current was only partly blocked by Cd, suggesting that there may be overlapping components that are dependent on Ca influx and Ca release from stores under these conditions.

There are several possible explanations why some investigators observe an $I_{Cl\text{-}2}$-like current and others do not. One explanation is that the ability to observe $I_{Cl\text{-}2}$ depends on the voltage protocol used. At holding potentials positive to −60 mV, activation of $I_{Cl\text{-}2}$ is small (Fig. 9). Furthermore, activation of $I_{Cl\text{-}2}$ requires larger amounts of IP_3 than activation of $I_{Cl\text{-}1}$ (unpublished data). In addition, the activation of Ca influx may require that the internal stores become sufficiently depleted. We have observed that with oocytes from some donors, $I_{Cl\text{-}2}$ induction is very small (~ 100 nA). If such an oocyte is placed in 0-Ca solution for ~30 s and then returned to normal Ca, $I_{Cl\text{-}2}$ becomes much larger (~ 1 μA) the instant the oocyte is returned to normal Ca. Thus, it seems that some oocytes are more efficient at recycling the Ca that is released in response to IP_3 such that the pools do not become depleted sufficiently to activate Ca influx. Some oocytes may lose cytosolic Ca more rapidly than others and this may determine the rate at which $I_{Cl\text{-}2}$ develops. Another possible consideration is that oocytes may differ in the number of follicular cells adhering to the oocyte. David Clapham (personal communication) has found that collagenase treatment of oocytes does not always completely remove the follicular cell layer. Thus, it is formally possi-

ble that some of the currents we have described here are due to adhering follicular cells that are attached by gap junctions to the oocyte. At the level of a high-quality dissecting microscope, we do not see any follicular cells, but a more detailed study would be required to adequately address this question.

Boton et al. (1989) have described two different Ca-activated Cl conductances in oocytes permeabilized with A23187. When the permeabilized oocytes were placed in solutions containing low Ca, only one kinetic component was observed, but addition of >2 mM Ca induced a current with two distinct kinetic components. The IV curves for both components determined by switching to Ca-containing solution at different holding potentials or by voltage ramps were linear between 0 and −60 mV, but exhibited a decreasing conductance at more negative potentials. This is similar to the steady-state IV relationship of $I_{Cl\text{-}1}$ described here, but it remains uncertain how these two components relate to $I_{Cl\text{-}1}$ and $I_{Cl\text{-}2}$. The two components differed with respect to their sensitivity to Ca, block by injection of EGTA, and extracellular application of the Cl-channel blocker 9-AC. Furthermore, the fast and slow components were inactivated to differing extents by Ca via a mechanism that may involve phosphorylation by protein kinase C (Boton et al., 1990; Petersen and Berridge, 1994). The two components of the current response to 5-HT or ACh could also be separated on the basis of sensitivity to EGTA suggesting that these two components may be mediated by different channels or pathways.

Mechanisms of $I_{Cl\text{-}2}$ Activation

Yao and Parker (1993) have suggested that the T_{in} current, which we propose is identical to $I_{Cl\text{-}2}$, arises because Ca influx triggers regenerative Ca release from IP_3-sensitive stores. It is known that Ca and IP_3 act synergistically in stimulating Ca release from IP_3-sensitive stores (Iino, 1990; Bezprozvanny et al., 1991). Yao and Parker (1993) used several pieces of data to support this hypothesis, but one important piece of evidence was that the Cl current continued to increase when the membrane was depolarized to arrest Ca influx (as in Fig. 7 *B*). Thus, they conclude that activating Ca must come from stores. However, this interpretation depends on their assumption that the Cl current consists of a single time- and voltage-independent component. However, we believe that the activating current upon depolarization is the time- and voltage-dependent activation of $I_{Cl\text{-}1}$. This point of view is supported by the observation that $I_{Cl\text{-}2}$ is stimulated by Ca influx even when the Ca stores have been completely depleted by thapsigargin and 0-Ca (Petersen and Berridge, 1994). It should be emphasized that this re-interpretation of the regulation of Cl currents does not suggest that regenerative Ca release from IP_3 sensitive pools does not exist under these conditions. However, the finding that Ca-green fluorescence and Cl currents do not correlate well (Yao and Parker, 1993) suggests that regardless of the mechanisms generating the Ca transients, the Cl channels do not simply respond to bulk cytosolic Ca concentration.

Petersen and Berridge (1994) suggest that the activation of the $I_{Cl\text{-}2}$-like current involves a positive feedback mechanism, because the current induced by addition of Ca to store-depleted oocytes produces a current that increases explosively with voltage in the range between −50 and −60 mV (see Fig. 4 *C*, in Petersen and Berridge, 1994). Their interpretation that this current has a positive feedback depends on their assumption that the current observed in the voltage range of −30 to 0 mV is the same current as that underlying the current in the range negative to −30 mV. However, as we have shown, the current in the range positive to −30 mV is $I_{Cl\text{-}1}$ whereas $I_{Cl\text{-}2D}$ activates only negative to −40 mV. Our interpretation is that $I_{Cl\text{-}2}$ is a voltage-dependent current that activates steeply with hyperpolarization in this range of potentials (Fig. 9 *B*).

In summary, there are two Ca-activated Cl currents in *Xenopus* oocytes. One of these is stimulated preferentially by Ca influx through store-operated channels, whereas the other can be activated by Ca released from stores or by Ca influx.

Dedicated to my father, who taught me how to use my hands. He died the day I submitted the final version of this manuscript, June 3, 1996.

I would like to thank Susan Mierergerd and Amber Rinderkneckt for preparing and injecting oocytes and Drs. Y. Hirayama, A. Ivanov, David Clapham, and Henry Lester for comments on the manuscript.

Supported by National Institutes of Health grants HL50474 and HI21195.

Original version received 16 April 1996 and accepted version received 5 June 1996.

REFERENCES

Barish, M.E. 1983. A transient calcium-dependent chloride current in the immature *Xenopus* oocyte. *J. Physiol. (Camb.).* 342:309–325.

Berridge, M.J. 1988. Inositol triphosphate-induced membrane potential oscillations in *Xenopus* oocytes. *J. Physiol. (Camb.).* 403:589–599.

Bezprozvanny, I., J. Watras, and B.E. Ehrlich. 1991. Bell-shaped calcium-response curves of Ins(1,4,5)P_3 and calcium-gated channels from endoplasmic reticulum of cerebellum. *Nature (Lond.).* 351: 751–754.

Boton, R., N. Dascal, B. Gillo, and Y. Lass. 1989. Two calcium-activated chloride conductances in *Xenopus laevis* oocytes permeabilized with the ionophore A23187. *J. Physiol. (Camb.).* 408:511–534.

Boton, R., D. Singer, and N. Dascal. 1990. Inactivation of calcium-activated chloride conductance in *Xenopus* oocytes: roles of calcium and protein kinase C. *Pflugers Arch.* 416:1–6.

Clapham, D. 1995. Calcium signaling. *Cell.* 80:259–268.

Dascal, N. 1987. The use of *Xenopus* oocytes for the study of ion channels. *CRC Crit. Rev. Biochem.* 22:317–387.

Dascal, N., E.M. Landau, and Y. Lass. 1984. *Xenopus* oocyte resting potential, muscarinic responses and the role of calcium and guanosine 3′,5′-cyclic monophosphate. *J. Physiol. (Camb.).* 352:551–574.

Dascal, N., T.P. Snutch, H. Lübbert, N. Davidson, and H.A. Lester. 1986. Expression and modulation of voltage-gated calcium channels after RNA injection in *Xenopus* oocytes. *Science (Wash. DC).* 231:1147– 1150.

DeLisle, S., D. Pittet, B.V.L. Potter, P.D. Lew, and M.J. Welsh. 1992. $InsP_3$ and $Ins(1,3,4,5)P_4$ act in synergy to stimulate influx of extracellular Ca^{2+} in *Xenopus* oocytes. *Am. J. Physiol.* 262:C1456–C1463.

Fasolato, C., B. Innocenti, and T. Pozzan. 1994. Receptor-activated Ca^{2+} influx: how many mechanisms for how many channels? *Trends Pharmacol. Sci.* 15:77–83.

Gillo, B., Y. Lass, E. Nadler, and Y. Oron. 1987. The involvement of inositol 1,4,5-triphosphate and calcium in the two-component response to acetylcholine in *Xenopus* oocytes. *J. Physiol. (Camb.).* 392:349–361.

Girard, S., and D. Clapham. 1993. Acceleration of intracellular calcium waves in *Xenopus* oocytes by calcium influx. *Science (Wash. DC).* 260:229–232.

Hodgkin, A.L., and A.F. Huxley. 1952. A quantitative description of membrane current and its application to conduction and excitation in nerve. *J. Physiol. (Camb.).* 117:500–544.

Hoth, M., and R. Penner. 1993. Calcium release-activated calcium current in rat mast cells. *J. Physiol. (Camb.).* 465:359–386.

Iino, M. 1990. Biphasic Ca^{2+}-dependence of inositol 1,4,5-trisphosphate-induced Ca release in smooth muscle cells of the guinea pig *Taenia caeci. J. Gen. Physiol.* 95:1103–1122.

Lechleiter, J.D., and D.E. Clapham. 1992. Molecular mechanisms of intracellular calcium excitability in *X. laevis* oocytes. *Cell.* 283: 294.

Lupu-Meiri, M., A. Beit-Or, S.B. Christensen, and Y. Oron. 1993. Calcium entry in *Xenopus* oocytes: effects of inositol trisphosphate, thapsigargin and DMSO. *Cell Calcium.* 14:101–110.

Meldolesi, J., E. Clementi, C. Fasolato, D. Zacchetti, and T. Pozzan. 1991. Ca^{2+} influx following receptor activation. *Trends Pharmacol. Sci.* 12:289–292.

Miledi, R. 1982. A calcium-dependent transient outward current in *Xenopus laevis* oocytes. *Proc. R. Soc. Lond. B Biol. Sci.* 215:491–497.

Miledi, R., I. Parker, and R.M. Woodward. 1989. Membrane currents elicited by divalent cations in *Xenopus* oocytes. *J. Physiol. (Camb.).* 417:173–195.

Miledi, R., and J. Parker. 1984. Chloride current induced by injection of calcium into *Xenopus* oocytes. *J. Physiol. (Camb.).* 357:173–183.

Morgan, A.J., and R. Jacob. 1994. Ionomycin enhances Ca^{2+} influx by stimulating store-regulated cation entry and not by a direct action at the plasma membrane. *Biochem. J.* 300:665–672.

Oron, Y.,N. Dascal, E. Nadler, and M. Lupu. 1985. Inositol 1,4,5-trisphosphate mimics muscarinic response in *Xenopus* oocytes. *Nature (Lond.).* 313:141–143.

Parekh, A.B., M. Foguet, H. Lubbert, and W. Stuhmer. 1993. Ca^{2+} oscillations and Ca^{2+} influx in *Xenopus* oocytes expressing a novel 5-hydroxytryptamine receptor. *J. Physiol. (Camb.).* 469:653–671.

Parker, I., C.B. Gundersen, and R. Miledi. 1985. A transient inward current elicited by hyperpolarization during serotonin activation in *Xenopus* oocytes. *Proc. R. Soc. Lond. B Biol. Sci.* 223:279–292.

Parker, I., and I. Ivorra. 1991. Inositol tetrakisphosphate liberates stored Ca^{2+} in *Xenopus* oocytes and facilitates responses to inositol trisphosphates. *J. Physiol. (Camb.).* 433:207–227.

Parker, I., and R. Miledi. 1986. Changes in intracellular calcium and in membrane currents evoked by injection of inositol trisphosphate into *Xenopus* oocytes. Proceedings of the Royal Society of London 228:307–315.

Parker, I., and R. Miledi. 1987. Inositol trisphosphate activates a voltage-dependent calcium influx in *Xenopus* oocytes. *Proc. R. Soc. Lond. B Biol. Sci.* 231:27–36.

Petersen, C.C.H., and M.J. Berridge. 1994. The regulation of capacitative calcium entry by calcium and protein kinase C in *Xenopus* oocytes. *J. Biol. Chem.* 269:32246–32253.

Pozzan, T., R. Rizzuto, P. Volpe, and J. Meldolesi. 1994. Molecular and cellular physiology of intracellular stores. *Physiol. Rev.* 74: 595–636.

Premack, B., T. McDonald, and P. Gardner. 1994. Activation of Ca^{2+} current in Jurkat T cells following the depletion of Ca^{2+} stores by microsomal Ca^{2+} -ATPase inhibitors. *J. Immunol.* 152: 5226–5240.

Putney, J.W. 1990. Capacitative calcium entry revisited. *Cell Calcium.* 11:611–624.

Putney, J.W. 1992. Inositol phosphates and calcium entry. *Adv. Second Messenger Phosphoprotein Res.* 26:143–160.

Putney, J.W. 1993. Excitement about calcium signalling in inexcitable cells. *Science (Wash. DC).* 262:676–678.

Snyder, P.M., K. Krause, and M.J. Welsh. 1988. Inositol triphosphate isomers, but not inositol 1,3,4,5-tetrakisphosphate, induce calcium influx in *Xenopus* laevis oocytes. *J. Biol. Chem.* 263:11048–11051.

Takemura, H., and J.W. Putney. 1989. Capacitative calcium entry in parotid acinar cells. *Biochem. J.* 258:409–412.

Tsien, R.W., and R.Y. Tsien. 1990. Calcium channels, stores, and oscillations. *Annu. Rev. Cell Biol.* 6:715–760.

White, M.M., and M. Aylwin. 1990. Niflumic and flufenamic acids are potent reversible blockers of Ca^{2+}-activated Cl^- channels in *Xenopus* oocytes. *Mol. Pharmacol.* 37:720–724.

Yao, Y., and I. Parker. 1993. Inositol trisphosphate-mediated Ca^{2+} influx into *Xenopus* oocytes triggers Ca^{2+} liberation from intracellular stores. *J. Physiol. (Camb.).* 468:275–296.

Zweifach, A., and R. Lewis. 1993. Mitogen-regulated Ca^{2+} current of T lymphocytes is activated by depletion of intracellular Ca^{2+} stores. *Proc. Natl. Acad. Sci. USA.* 90:6295–6299.